R. & M. No. 2948
(16,153)
A.R.C. Technical Report

MINISTRY OF SUPPLY

AERONAUTICAL RESEARCH COUNCIL
REPORTS AND MEMORANDA

Interference Corrections for Asymmetrically Loaded Wings in Closed Rectangular Wind Tunnels

By

H. C. GARNER, B.A., and W. E. A. ACUM, A.R.C.S., B.Sc.,
of the Aerodynamics Division, N.P.L.

LONDON: HER MAJESTY'S STATIONERY OFFICE
1957
ELEVEN SHILLINGS NET

Interference Corrections for Asymmetrically Loaded Wings in Closed Rectangular Wind Tunnels

By

H. C. Garner, B.A., and W. E. A. Acum, A.R.C.S., B.Sc.,
of the Aerodynamics Division, N.P.L.

Reports and Memoranda No. 2948†
September, 1953

Summary.—The problem of tunnel interference on a complete lifting wing fitted with ailerons is considered in relation to aerodynamic measurements on a six-component balance. Asymmetric loading introduces corrections to the incidence of the wing, the drag and the rolling, pitching and yawing moments.

The basic theory of wall interference in closed rectangular tunnels is outlined in sections 3 to 5. In section 6, the tunnel-induced upwash is expressed in terms of the loading on the wing and four quantities dependent on the shape of tunnel. These quantities are evaluated for a duplex tunnel ($b = 2h$) in Tables 4 to 7 and may be computed for a general rectangular shape with the aid of Tables 1 to 3.

Section 7 describes how the evaluation of tunnel interference is conveniently linked with Multhopp's lifting-surface theory to determine corrections to incidence, pitching moment and rolling moment. A worked example in the case of antisymmetrical loading is given in Appendix II, which concludes with an approximate procedure, suggested as a possible substitute for the lifting-surface method.

The corrections to drag and yawing moment are discussed in detail in section 8. All the corrections are summarized in section 9 and expressed as products of experimental aerodynamic coefficients and theoretically determined quantities, which are evaluated in Table 8 for an arrowhead wing (Fig. 4) with various ailerons in a duplex tunnel.

The corrections to incidence due to symmetrical loading are equivalent to corrections to lift of the opposite signs these vary from -11 to $-5\frac{1}{2}$ per cent depending on the type of loading. The corresponding corrections to rolling moment due to antisymmetrical loading are about -2 per cent. Corrections to drag are very roughly $+20$ per cent. When the spanwise loading is asymmetrical, there arises an induced yawing moment, which may require an interference correction of the order $+25$ per cent.

---

1. *Introduction.*—The present work has arisen in connection with some six-component balance measurements at low speed on a complete model of an uncambered arrowhead wing fitted with various aileron surfaces. The plan-form, shown in Fig. 4, is fairly large in relation to the National Physical Laboratory Duplex Wind Tunnel, in which the tests have been carried out, so that calculations of tunnel-wall interference are required to a fair degree of accuracy. The general theory of tunnel interference due to lift is well known, but the authors are unaware of a ready means of calculating the tunnel-induced rolling moments and yawing moments due to an arbitrary asymmetrical loading on a swept wing of moderately low aspect ratio.

---

†Published with the permission of the Director, National Physical Laboratory.

The corresponding problem of symmetrical loading has been considered in Ref. 1 (Acum, 1950), where tables of parameters δ_0 and δ_1 are available for four tunnels of closed rectangular section. Convenient approximate methods of using these tables to compute the interference on symmetrical models with control surfaces or half-models mounted on one wall of a tunnel are described in sections 4.4, 4.5 and 4.6 of Ref. 2 (Bryant and Garner, 1950). The counterpart for antisymmetrical loading is now required. Graham[3] (1945) has considered this problem for an unswept lifting line with uniform loading along the span of a deflected aileron. Although he has shown that the magnitude of the interference is not large, his representation is not suitable for the present investigation. Reference should also be made to a general survey of wall interference in closed rectangular tunnels by Sanders and Pounder[4] (1949), who give a full mathematical analysis of the extension of two-dimensional results to three dimensions by means of lifting-line theory.

Without recourse to lifting-surface theory[9] (Multhopp, 1950), the problem of deducing tunnel interference from balance measurements alone is difficult in the case of antisymmetrical loading. The loading characteristics of a wing must be related to the coefficients of lift, rolling moment and pitching moment, C_L, C_l and C_m respectively, which are assumed to have been measured. From the following table, it will be apparent that, for a given ratio of model span to tunnel breadth the magnitude of the interference and the amount of relevant information vary rather similarly with the arrangement of the model. In the antisymmetrical problem the need for less accuracy, because the interference is not large, is offset by the fact that the single balance measurement C_l does not determine the chordwise or the spanwise centre of pressure on one half of the wing. Approximate values of both these co-ordinates are desirable when carrying out calculations of tunnel interference.

Arrangement of model	Relevant balance measurements	Tunnel-wall interference
Half-wing adjacent to tunnel	C_L, C_l, C_m,	Rather large
Symmetrically loaded wing	C_L, C_m,	Moderate
Antisymmetrically loaded wing	C_l,	Rather small

In this report a continuous loading over an arbitrary plan-form will be specified by the local lift and the local chordwise centre of pressure. The tunnel-induced upwash due to the system of images of a bound vortex concentrated along the locus of the local centres of pressure with its wake of trailing vorticity is expressed as a spanwise integral involving the quantities P_0, P_1, Q_0 and Q_1. Q_0 and Q_1 are the differential coefficients of the quantities δ_0 and δ_1 tabulated in Ref. 1, but have been obtained here directly. The method of obtaining P_1 and Q_1 gives mathematical expressions that are very convenient for computation.

The effect of tunnel-induced upwash is determined on the basis of Multhopp's[9] lifting-surface theory. When basic calculations by Ref. 9 are available for the particular plan-form, the computation of forces and moments corresponding to the tunnel-induced upwash is more convenient than that envisaged in Refs. 1 and 2. The antisymmetrical problem arising from the tests in the N.P.L. Duplex Wind Tunnel is solved as an illustrative example in Appendix II. This is followed by a suggestion as to what can best be done by approximate means when no lifting-surface theory is available.

The quantities P_0, P_1, Q_0 and Q_1 are tabulated for the Duplex Tunnel, but the general functions in Tables 1, 2 and 3 are included, so that corresponding quantities can readily be obtained for any other closed rectangular tunnel.

2. *List of Symbols*.—

A	Aspect ratio $(2s/\bar{c})$
a_1, a_2	Equivalent two-dimensional $\partial C_L/\partial \alpha$, $\partial C_L/\partial \xi$
b	Tunnel breadth
C_D, C_D'	Free stream, measured drag$/\frac{1}{2}\rho V^2 S$
C_L, C_L'	Free stream, measured lift$/\frac{1}{2}\rho V^2 S$
C_l, C_l'	Free stream, measured rolling moment$/\frac{1}{2}\rho V^2 S.2s$
C_m, C_m'	Free stream, measured pitching moment$/\frac{1}{2}\rho V^2 S\bar{c}$
C_n, C_n'	Free stream, measured yawing moment$/\frac{1}{2}\rho V^2 S.2s$
c, c_0, $\bar{c}$	Local, root, mean wing chord
E	Ratio of aileron chord to wing chord
$F(\lambda)$	*See* equation (5.6) and Appendix I
$f(\lambda)$	*See* equation (5.2) and Appendix I
f_1, f_2, f_3, f_4	*See* equations (6.3), (6.7) and Tables 1 and 2
h	Tunnel height
I, J	*See* equations (7.1), (8.4), (8.5)
$K(t)$	Strength of basic vortex system (section 3)
K_0, K_1	Bessel functions (Ref. 10)
l_2	Two-dimensional centre of pressure $[(x_{c.p.} - x_l)/c]$
m	Number of wing sections taken into account (Ref. 9)
P_0, P_1	*See* equations (6.4), (6.8)
Q_0, Q_1	*See* equations (6.5), (6.9)
S	Area of plan-form of wing
s	Semi-span of wing
t	Semi-width of basic vortex system
V	Velocity of free stream
w	Upwash induced by tunnel interference
$X_{c.p.}$	Local chordwise centre of pressure $[(x_{c.p.} - x_l)/c]$
(x, y, z)	Rectangular co-ordinates, streamwise, spanwise, upwards
$x_0(t)$	Locus of lifting line in equation (7.2)
x_l, x_t	Leading, trailing edge
$y_a < y < s$	Spanwise extent of aileron
α	Incidence of wing
Γ	Circulation round wing
γ	Non-dimensional circulation $(\Gamma/2sV)$
δ_0, δ_1	*See* equation (3.1)

List of Symbols—continued.

η	Non-dimensional spanwise co-ordinate, y/b
θ	Angular spanwise co-ordinate, $y = s \cos \theta$
Λ	Angle of sweepback of quarter-chord line
λ	Taper ratio of wing (Appendix II)
λ	Real independent variable, used in definitions of functions and tables
μ	Ratio h/b ($= \frac{1}{2}$ for a duplex tunnel)
μ	Non-dimensional local pitching moment, $cC_m/4s$ (section 7 and Appendix II)
ξ	Angular deflection of aileron
σ	Non-dimensional semi-span of wing, s/b
τ	Non-dimensional semi-width of basic vortex system, t/b
ϕ_0, ψ_0	*See* equations (6.4), (6.5)
ϕ_1, ψ_1	*See* equations (6.8), (6.9)
Prefix δ	denotes effect of tunnel interference
Prefix Δ	denotes interference correction to be applied
Superscript $'$	denotes experimental aerodynamic coefficient (corrected for tunnel blockage only)
Superscript $'$ or $''$	denotes value of x at solving point (Ref. 9)
Suffix $\frac{3}{4}$	denotes value of $\delta\alpha$ at local three-quarter chord
Suffix a	denotes antisymmetrical loading
Suffix s	denotes symmetrical loading
Suffix n or ν	denotes spanwise station $y_n = s \sin \dfrac{n\pi}{m+1}$ or $y_\nu = s \sin \dfrac{\nu\pi}{m+1}$.

---

3. *Basic Representation.*—Consider a closed rectangular wind tunnel containing a model wing with deflected ailerons such that the spanwise distribution of lift is antisymmetrical with respect to the vertical plane of symmetry of the tunnel. It will be assumed that the wing can be regarded as a vortex sheet in the horizontal plane of symmetry of the tunnel. The co-ordinates are referred to axes Ox in the direction of flow, Oy spanwise and Oz upwards. The elementary vortex system, shown in Fig. 1, is referred to an origin O at the centre of a particular cross-section of the tunnel and consists of trailing vortices along the lines $y = \pm t$, $z = 0$, both of strength $+ K(0 < x < \infty)$, and a bound vortex along the line $x = 0$, $z = 0$, of strength $- K(- t < y < 0)$ and $+ K(0 < y < t)$.

This vorticity distribution has an abrupt discontinuity at the point O and so is physically unreal. However when a similar system of equal and opposite strength and of width $2(t - \delta t)$ is superposed, the resulting vortex system corresponds to two equal and opposite horse-shoe vortices of width δt and circulation K symmetrically situated in the tunnel. Any antisymmetrical wing loading can be built up from elements of this kind. If, therefore, the tunnel-induced upwash due to the vortex system of Fig. 1 can be determined, it will be possible to calculate the interference for any wing with antisymmetrical lift.

By the usual procedure for rectangular tunnels the interference may be regarded as that due to an image system of vortices outside the tunnel. A doubly infinite array is necessary to give streamline flow along the walls of the tunnel; and a cross-section of this system far downstream is shown in Fig. 2. The strengths of the vortices alternate in sign both horizontally and vertically. The interference in the plane $z = 0$ due to the basic vortex system is expressed as an angle of upwash

$$\frac{w}{V} = \frac{w}{V}(x, y\,;\; t, K)$$
$$= \frac{4Kt}{Vbh}\left\{\delta_0(y, t) + \frac{x}{h}\delta_1(y, t) + 0\left(\frac{h}{x}\right)^3\right\}, \qquad (3.1)$$

where, as in the symmetrical theory of Ref. 1, $\delta_0(y, t)$ and $\delta_1(y, t)$ are the functions to be determined and the terms involving the third and higher powers of x/h are neglected.

4. *Formulae for* $\delta_0(y, t)$. $\delta_0(y, t)$ represents the upwash at a point $(0, y, 0)$ due to the image system of the elementary vortex (K, t) in Fig. 1. The well known theorem of Prandtl shows that in the limit as $x \to \infty$ equation (3.1) becomes

$$\left(\frac{w}{V}\right)_\infty = \frac{4Kt}{Vbh}\{2\delta_0(y, t)\}, \qquad (4.1)$$

which may be evaluated from the image system in Fig. 2 on a two-dimensional basis. Consider the vertical column of vortices of strengths $(-1)^n K$ at positions $(y, z) = (t, nh)(-\infty < n < \infty)$. The upwash at the point $(y, 0)$ due to this column is

$$w = \frac{1}{2\pi}\sum_{n=-\infty}^{\infty}(-1)^n K\frac{y - t}{(y - t)^2 + n^2h^2}$$
$$= \frac{K}{2\pi(y - t)} + \frac{K}{\pi h}\sum_{n=1}^{\infty}(-1)^n\frac{\lambda}{n^2 + \lambda^2},$$

where $\lambda = (y - t)/h$.

Now †

$$\sum_{n=1}^{\infty}(-1)^n\frac{\lambda}{n^2 + \lambda^2} = \tfrac{1}{2}\left\{\pi \operatorname{cosech} \pi\lambda - \frac{1}{\lambda}\right\}.$$

Hence

$$w = \frac{K}{2h}\operatorname{cosech}\frac{\pi(y - t)}{h}. \qquad (4.2)$$

It follows from equation (4.2) that the upwash due to all the vortices, indicated in Fig. 2 and including those inside the tunnel, is

$$\frac{K}{2h}\sum_{m=-\infty}^{\infty}(-1)^m\left\{\operatorname{cosech}\frac{\pi(y - mb - t)}{h} + \operatorname{cosech}\frac{\pi(y - mb + t)}{h}\right\}.$$

To obtain the upwash due to the image system, the contributions of the two vortices inside the tunnel are removed, so that

$$\left(\frac{w}{V}\right)_\infty = \frac{K}{2Vh}\left[-\frac{h}{\pi(y \pm t)} + \sum_{m=-\infty}^{\infty}(-1)^m \operatorname{cosech}\frac{\pi(y \pm t - mb)}{h}\right]. \qquad (4.3)$$

†This follows from the formula $\pi/\sin \pi\lambda = 1/\lambda - 2\lambda \sum_{n=1}^{\infty} (-1)^n/(n^2 - \lambda^2)$, proved in *Theory and Application of Infinite Series* by K. Knopp (p. 208).

On equating (4.1) and (4.3), it follows that the antisymmetrical horse-shoe vortex in Fig. 1 causes on the axis Oy a tunnel-induced upwash represented by

$$\delta_0(\eta, \tau) = \frac{1}{16\tau}\left[-\frac{\mu}{\pi(\eta \pm \tau)} + \sum_{m=-\infty}^{\infty} (-1)^m \operatorname{cosech}\frac{\pi}{\mu}(\eta \pm \tau - m)\right], \quad \ldots \quad \ldots \quad (4.4)$$

where $\eta = y/b$, $\tau = t/b$, $\mu = h/b$.

In the case of a symmetrical horse-shoe vortex, by changing the sign of the appropriate terms a similar analysis gives

$$\delta_0(\eta, \tau) = \frac{1}{16\tau}\left[-\frac{\mu}{\pi(\eta - \tau)} + \sum_{m=-\infty}^{\infty} \operatorname{cosech}\frac{\pi}{\mu}(\eta - \tau - m) + \frac{\mu}{\pi(\eta + \tau)} - \sum_{n=-\infty}^{\infty} \operatorname{cosech}\frac{\pi}{\mu}(\eta + \tau - m)\right]. \quad \ldots \quad \ldots \quad \ldots \quad (4.5)$$

5. *Formulae for* $\delta_1(y, t)$. $\delta_1(y, t)$ represents the gradient of the upwash in the direction of the undisturbed flow at a point $(0, y, 0)$ due to the image system of the elementary vortex (K, t) in Fig. 1. The trailing and bound vorticity will be considered separately.

From the results of Ref. 5, section 12.2, the upwash at a point (x, y, z) due to a vortex of strength K extending along the positive x-axis is

$$w_t = \frac{Ky}{4\pi(y^2 + z^2)}\left\{1 + \frac{x}{\sqrt{(x^2 + y^2 + z^2)}}\right\}. \quad \ldots \quad \ldots \quad \ldots \quad \ldots \quad (5.1)$$

Hence

$$\frac{d}{dx}\left(\frac{w_t}{V}\right) = \frac{Ky}{4\pi V}(x^2 + y^2 + z^2)^{-3/2}$$

$$= \frac{K}{4\pi V}\frac{y}{(y^2 + z^2)^{3/2}}, \text{ when } x = 0.$$

For a vertical column of such vortices of alternating sign and containing those at the wing

$$\frac{d}{dx}\left(\frac{w_t}{V}\right) = \frac{K}{4\pi V}\left[\frac{y}{|y|^3} + 2\sum_{n=1}^{\infty}(-1)^n \frac{y}{(y^2 + n^2h^2)^{3/2}}\right]$$

$$= \frac{K}{4\pi Vh^2} f(y/h), \quad \ldots \quad \ldots \quad \ldots \quad \ldots \quad \ldots \quad \ldots \quad \ldots \quad \ldots \quad (5.2)$$

where

$$f(\lambda) = \frac{\lambda}{|\lambda|^3} + 2\sum_{n=1}^{\infty}(-1)^n \frac{\lambda}{(n^2 + \lambda^2)^{3/2}}.$$

Then it follows, as in section 4, that the contribution to $d(w/V)/dx$ due to the images of the trailing vorticity is

$$\frac{d}{dx}\left(\frac{w_t}{V}\right) = \frac{K}{4\pi Vh^2}\left[-\frac{\mu^2(\eta \pm \tau)}{|\eta \pm \tau|^3} + \sum_{m=-\infty}^{\infty}(-1)^m f\left(\frac{\eta \pm \tau - m}{\mu}\right)\right]. \quad \ldots \quad \ldots \quad (5.3)$$

Now consider one half of the bound vortex along the line $x = 0$, $z = 0$ of strength $K(0 < y < t)$. From Ref. 5, section 12.2, the upwash due to this vortex at a point (x, y, z) is

$$w_1 = -\frac{K}{4\pi}\frac{x}{x^2+z^2}\left\{\frac{y}{\sqrt{\{x^2+y^2+z^2\}}}-\frac{y-t}{\sqrt{\{x^2+(y-t)^2+z^2\}}}\right\}. \quad .. \quad (5.4)$$

Hence, in the limit as $x \to 0$,

$$\frac{d}{dx}\left(\frac{w_1}{V}\right) = -\frac{K}{4\pi V}\frac{1}{z^2}\left\{\frac{y}{\sqrt{\{y^2+z^2\}}}-\frac{y-t}{\sqrt{\{(y-t)^2+z^2\}}}\right\}.$$

To obtain the upwash w_2 corresponding to the other half of the bound vorticity $(-t < y < 0)$, y is replaced by $(y + t)$ and the sign of K is changed. Thus

$$\frac{d}{dx}\left(\frac{w_2}{V}\right) = \frac{K}{4\pi V}\frac{1}{z^2}\left\{\frac{y+t}{\sqrt{\{(y+t)^2+z^2\}}}-\frac{y}{\sqrt{\{y^2+z^2\}}}\right\}.$$

Hence the vertical column containing the total bound vorticity at the wing and its images of alternating sign contributes

$$\frac{d}{dx}\left(\frac{w_b}{V}\right) = \frac{K}{4\pi V}\sum_{n=-\infty}^{\infty}\frac{(-1)^n}{n^2h^2}\left\{\frac{y-t}{\sqrt{\{(y-t)^2+n^2h^2\}}}+\frac{y+t}{\sqrt{\{(y+t)^2+n^2h^2\}}}-\frac{2y}{\sqrt{\{y^2+n^2h^2\}}}\right\}, \quad (5.5)$$

where the term $n = 0$ corresponding to the wing itself is infinite when $-t \leqslant y \leqslant t$ and otherwise tends to the finite limit

$$\frac{K}{4\pi V}\left\{\frac{y}{|y|^3}-\frac{y-t}{2|y-t|^3}-\frac{y+t}{2|y+t|^3}\right\}.$$

Therefore, from a single column of images,

$$\frac{d}{dx}\left(\frac{w_b}{V}\right) = \frac{K}{4\pi V h^2}\left\{F\left(\frac{\eta-\tau}{\mu}\right)+F\left(\frac{\eta+\tau}{\mu}\right)-2F\left(\frac{\eta}{\mu}\right)\right\}, \quad .. \quad .. \quad .. \quad (5.6)$$

where

$$F(\lambda) = -\frac{\lambda}{2|\lambda|^3}+2\sum_{n=1}^{\infty}\frac{(-1)^n}{n^2}\frac{\lambda}{\sqrt{(n^2+\lambda^2)}},$$

except that the first term is omitted when the column contains the wing. Then it follows, as in section 4, that the contribution to $d(w/V)/dx$ due to the images of the bound vorticity is

$$\begin{aligned}\frac{d}{dx}\left(\frac{w_b}{V}\right) = \frac{K}{4\pi V h^2}\Bigg[&\frac{\mu^2(\eta-\tau)}{2|\eta-\tau|^3}+\frac{\mu^2(\eta+\tau)}{2|\eta+\tau|^3}-\frac{\mu^2\eta}{|\eta|^3}\\ &+\sum_{m=-\infty}^{\infty}(-1)^m\left\{F\left(\frac{\eta-\tau-m}{\mu}\right)\right.\\ &\left.+F\left(\frac{\eta+\tau-m}{\mu}\right)-2F\left(\frac{\eta-m}{\mu}\right)\right\}\Bigg]. \quad .. \quad .. \quad .. \quad .. \quad (5.7)\end{aligned}$$

By combining equations (5.3) and (5.7) it may be seen that the image system of the elementary vortex (K, t) in Fig. 1 induces a gradient of upwash

$$\frac{d}{dx}\left(\frac{w}{V}\right) = \frac{d}{dx}\left(\frac{w_t}{V}\right) + \frac{d}{dx}\left(\frac{w_b}{V}\right)$$

$$= \frac{K}{4\pi Vh^2}\left[-\frac{\mu^2(\eta - \tau)}{2|\eta - \tau|^3} - \frac{\mu^2(\eta + \tau)}{2|\eta + \tau|^3} - \frac{\mu^2\eta}{|\eta|^3}\right.$$

$$+ \sum_{m=-\infty}^{\infty} (-1)^m \left\{f\left(\frac{\eta \pm \tau - m}{\mu}\right)\right.$$

$$\left.\left. + F\left(\frac{\eta \pm \tau - m}{\mu}\right) - 2F\left(\frac{\eta - m}{\mu}\right)\right\}\right] \qquad \text{(5.8)}$$

in the limit as $x \to 0$. On comparing equations (3.1) and (5.8), it will be seen that

$$\delta_1(\eta, \tau) = \frac{1}{16\pi\tau}\left[-\frac{\mu^2(\eta - \tau)}{2|\eta - \tau|^3} - \frac{\mu^2(\eta + \tau)}{2|\eta + \tau|^3} - \frac{\mu^2\eta}{|\eta|^3} + \sum_{m=-\infty}^{\infty} (-1)^m \left\{f\left(\frac{\eta \pm \tau - m}{\mu}\right)\right.\right.$$

$$\left.\left. + F\left(\frac{\eta \pm \tau - m}{\mu}\right) - 2F\left(\frac{\eta - m}{\mu}\right)\right\}\right], \qquad \text{(5.9)}$$

where $\eta = y/b$, $\tau = t/b$ and $\mu = h/b$.

In the case of a symmetrical wing, by a similar analysis

$$\delta_1(\eta, \tau) = \frac{1}{16\pi\tau}\left[-\frac{\mu^2(\eta - \tau)}{2|\eta - \tau|^2} + \sum_{m=-\infty}^{\infty}\left\{f\left(\frac{\eta - \tau - m}{\mu}\right) + F\left(\frac{\eta - \tau - m}{\mu}\right)\right\}\right.$$

$$\left. + \frac{\mu^2(\eta + \tau)}{2|\eta + \tau|^3} - \sum_{m=-\infty}^{\infty}\left\{f\left(\frac{\eta + \tau - m}{\mu}\right) + F\left(\frac{\eta + \tau - m}{\mu}\right)\right\}\right]. \qquad \text{(5.10)}$$

6. *Calculation of P_0, P_1, Q_0 and Q_1.*—For the purpose of calculating tunnel interference, it is assumed that the bound vorticity may be concentrated along the line $x = x_0(t)$ through the local centres of pressure, as indicated in Fig. 4. Suppose that the circulation round the wing at any chordwise section is $\Gamma = \Gamma(t)$. When the loading is antisymmetrical, the interference due to the parts of the wing $-(t + \delta t) < y < -t$ and $t < y < (t + \delta t)$ is represented by the equal and opposite pair of horse-shoe vortices shown in Fig. 4. It follows from section 3 that the image system of these vortices contributes

$$\delta\left(\frac{w}{V}\right) = \frac{4\Gamma(t)}{Vbh}\left\{(t + \delta t)\,\delta_0(y, t + \delta t) - t\,\delta_0(y, t)\right.$$

$$\left. + \frac{x - x_0(t)}{h}\{(t + \delta t)\,\delta_1(y, t + \delta t) - t\,\delta_1(y, t)\}\right\}$$

$$= \frac{4\Gamma(\tau)}{Vh}\left[\frac{\partial}{\partial\tau}\{\tau\delta_0(\eta, \tau)\} + \frac{x - x_0(\tau)}{h}\frac{\partial}{\partial\tau}\{\tau\delta_1(\eta, \tau)\}\right]\delta\tau + O[(\delta\tau)^2].$$

Then for an antisymmetrically loaded wing the integrated tunnel-induced angle of upwash is expressed as

$$\frac{w}{V} = \int_0^{\sigma} \frac{4\Gamma(\tau)}{Vh}\left\{P_0(\eta, \tau) + \frac{x - x_0(\tau)}{h}\,P_1(\eta, \tau)\right\} d\tau\,, \qquad \text{(6.1)}$$

where

$$\sigma = s/b = \text{wing semi-span/tunnel breadth,}$$

$$P_0(\eta, \tau) = \frac{\partial}{\partial \tau}\{\tau \delta_0(\eta, \tau)\}, \quad \delta_0 \text{ being given in equation (4.4),}$$

$$P_1(\eta, \tau) = \frac{\partial}{\partial \tau}\{\tau \delta_1(\eta, \tau)\}, \quad \delta_1 \text{ being given in equation (5.9).}$$

Similarly for a symmetrically loaded wing

$$\frac{w}{V} = \int_0^\sigma \frac{4\Gamma(\tau)}{Vh}\left\{Q_0(\eta, \tau) + \frac{x - x_0(\tau)}{h} Q_1(\eta, \tau)\right\} d\tau \,, \qquad \text{(6.2)}$$

where

$$Q_0(\eta, \tau) = \frac{\partial}{\partial \tau}\{\tau \delta_0(\eta, \tau)\}, \quad \delta_0 \text{ being given in equation (4.5),}$$

$$Q_1(\eta, \tau) = \frac{\partial}{\partial \tau}\{\tau \delta_1(\eta, \tau)\}, \quad \delta_1 \text{ being given in equation (5.10).}$$

The quantities P_0 and Q_0 are easily calculated. From equations (4.4) and (6.1)

$$P_0(\eta, \tau) = \frac{1}{16}\frac{\partial}{\partial \tau}\left[-\frac{\mu}{\pi(\eta - \tau)} + \sum_{m=-\infty}^{\infty}(-1)^m \operatorname{cosech}\frac{\pi}{\mu}(\eta - \tau - m)\right.$$
$$\left. - \frac{\mu}{\pi(\eta + \tau)} + \sum_{m=-\infty}^{\infty}(-1)^m \operatorname{cosech}\frac{\pi}{\mu}(\eta + \tau - m)\right].$$

Then in terms of the functions

$$\left.\begin{aligned} f_1(\lambda) &= \frac{d}{d\lambda}\{\operatorname{cosech} \pi\lambda\} \\ f_2(\lambda) &= \frac{d}{d\lambda}\left\{\operatorname{cosech} \pi\lambda - \frac{1}{\pi\lambda}\right\} \end{aligned}\right\}, \qquad \text{(6.3)}$$

$$P_0(\eta, \tau) = \frac{1}{16\mu}\{\phi_0(\eta - \tau) - \phi_0(\eta + \tau)\} \,, \qquad \text{(6.4)}$$

where

$$\phi_0(\eta) = -f_2(\eta/\mu) - \sum_{m=1}^{\infty}(-1)^m\left\{f_1\left(\frac{\eta - m}{\mu}\right) + f_1\left(\frac{\eta + m}{\mu}\right)\right\}.$$

Similarly from equations (4.5) and (6.2),

$$Q_0(\eta, \tau) = \frac{1}{16\mu}\{\psi_0(\eta - \tau) + \psi_0(\eta + \tau)\} \,, \qquad \text{(6.5)}$$

where

$$\psi_0(\eta) = -f_2(\eta/\mu) - \sum_{m=1}^{\infty}\left\{f_1\left(\frac{\eta - m}{\mu}\right) + f_1\left(\frac{\eta + m}{\mu}\right)\right\}.$$

Since $f_1(\lambda)$ and $f_2(\lambda)$ are even functions of λ, it will be seen that $\phi_0(-\eta) = \phi_0(\eta)$ and $\psi_0(-\eta) = \psi_0(\eta)$. Values of $f_1(\lambda)$ and $f_2(\lambda)$ for positive λ are given in Table 1, whence it is clear that $\phi_0(\eta)$ and $\psi_0(\eta)$ are in the form of rapidly convergent series. By this means it is simple to calculate $P_0(\eta, \tau)$ and $Q_0(\eta, \tau)$.

The expressions for $\delta_1(\eta, \tau)$ in equations (5.9) and (5.10) are rather complicated. In earlier work[6] (Brown, 1938), the method of evaluation was to sum the contributions from all the images within a rectangle with the tunnel at its centre and to make a rough estimate of the effect of the remaining images. Among such methods, Ref. 6 and Appendix II to Ref. 2 probably give the most convenient approximations. These methods are not rapidly convergent, especially when the ratio $\mu = h/b$ is rather small. Olver[7] (1949), has established a transformation which converts the double series into a rapidly convergent and easily computable form ; and a similar transformation is used in section 3.2 of Ref. 4. The functions $f(\lambda)$ and $F(\lambda)$ in equations (5.2) and (5.6) are considered in Appendix I, where by a treatment similar to that of Ref. 7 it is shown that

$$\lambda \frac{dF}{d\lambda} = f(\lambda) = 4\pi\{K_1(\pi\lambda) + 3K_1(3\pi\lambda) + 5K_1(5\pi\lambda) + \ldots\}, \qquad (6.6)$$

where K_1 denotes the modified Bessel function[10] (Watson). Since these functions of a single variable are readily evaluated, the following method is believed to be the most convenient for general computation of P_1 and Q_1.

From equations (5.9) and (6.1),

$$P_1(\eta, \tau) = \frac{1}{16\pi}\frac{\partial}{\partial\tau}\left[-\frac{\mu^2(\eta-\tau)}{|\eta-\tau|^3} + \sum_{m=-\infty}^{\infty}(-1)^m\left\{f\left(\frac{\eta-\tau-m}{\mu}\right) + F\left(\frac{\eta-\tau-m}{\mu}\right)\right\}\right.$$
$$\left. - \frac{\mu^2(\eta+\tau)}{|\eta+\tau|^3} + \sum_{m=-\infty}^{\infty}(-1)^m\left\{f\left(\frac{\eta+\tau-m}{\mu}\right) + F\left(\frac{\eta+\tau-m}{\mu}\right)\right\}\right].$$

Then in terms of the functions

$$\left.\begin{aligned} f_3(\lambda) &= \frac{d}{d\lambda}\{f(\lambda) + F(\lambda)\} \\ f_4(\lambda) &= \frac{d}{d\lambda}\left\{f(\lambda) + F(\lambda) - \frac{\lambda}{2|\lambda|^3}\right\} \end{aligned}\right\}, \qquad (6.7)$$

$$P_1(\eta, \tau) = \frac{1}{16\pi\mu}\{\phi_1(\eta-\tau) - \phi_1(\eta+\tau)\}, \qquad (6.8)$$

where

$$\phi_1(\eta) = -f_4(\eta/\mu) - \sum_{m=1}^{\infty}(-1)^m\left\{f_3\left(\frac{\eta-m}{\mu}\right) + f_3\left(\frac{\eta+m}{\mu}\right)\right\}.$$

Similarly, for a symmetrically loaded wing, from equations (5.10) and (6.2),

$$Q_1(\eta, \tau) = \frac{1}{16\pi\mu}\{\psi_1(\eta-\tau) + \psi_1(\eta+\tau)\}, \qquad (6.9)$$

where

$$\psi_1(\eta) = -f_4(\eta/\mu) - \sum_{m=1}^{\infty}\left\{f_3\left(\frac{\eta-m}{\mu}\right) + f_3\left(\frac{\eta+m}{\mu}\right)\right\}.$$

Both $f(\lambda)$ and $F(\lambda)$ are odd functions of λ ; and the even functions $f_3(\lambda)$ and $f_4(\lambda)$ in equation (6.7) have been calculated from equation (6.6) by the Mathematics Division of the N.P.L. and are given for positive values of λ in Table 2. Like $f_1(\lambda)$ in Table 1, $f_3(\lambda)$ in Table 2 decreases rapidly as λ increases and is negligible when $\lambda > 5$. Thus the expressions $\phi_1(-\eta) = \phi_1(\eta)$ and $\psi_1(-\eta) = \psi_1(\eta)$ in equations (6.8) and (6.9) are rapidly convergent, so that $P_1(\eta, \tau)$ and $Q_1(\eta, \tau)$ are easily calculated.

Values of P_0, P_1, Q_0, Q_1 for a duplex tunnel ($\mu = \frac{1}{2}$) are given in Tables 4, 5, 6, 7 respectively. Similar calculations for other values of $\mu = h/b$ might involve interpolation in the values of the functions $f_1(\lambda)$, $f_2(\lambda)$, $f_3(\lambda)$, $f_4(\lambda)$ in Tables 1 and 2. f_1 and f_2 are readily evaluated from equation (6.3); and f_3 in equation (6.7) is easily obtained by subtracting $1/\lambda^3$ from f_4. Table 3 has been prepared so that with the use of second differences the values of $f_4(\lambda)$ may be obtained to an accuracy of $\pm 0{\cdot}0001$ (Appendix I).

7. *Evaluation of Tunnel Interference.*—In sections 3 to 6, the tunnel interference due to a lifting surface is expressed as an angle of upwash $w/V = \delta\alpha$, which may be calculated at any position in the supposedly horizontal plane of the model. From equation (6.1), when the spanwise loading is antisymmetrical,

$$\delta\alpha(x, y) = I + \frac{x}{h} J \, , \qquad \qquad (7.1)$$

where

$$I = \frac{8s^2}{bh} \int_0^1 \gamma \left\{ P_0 - \frac{x_0}{h} P_1 \right\} d(\tau/\sigma) \, ,$$

$$J = \frac{8s^2}{bh} \int_0^1 \gamma P_1 \, d(\tau/\sigma) \, ,$$

x is conveniently measured from the leading apex of the wing (Fig. 4),

$y = b\eta$,

$s = b\sigma$,

$\gamma = \Gamma/2sV$ is the non-dimensional circulation at the section $t = b\tau$,

P_0, P_1 are functions of η and τ for a given rectangular tunnel (section 6),

and

(x_0, t) are the co-ordinates of the chordwise centre of pressure.

In the case of the six-component balance measurements on a complete model (section 1), the only experimental quantity relevant to equation (7.1) is C_l', the measured coefficient of rolling moment corrected only for tunnel blockage (Ref. 2, section 4.1). Provided that γ/C_l' and x_0 are known as functions of τ/σ, it is possible to evaluate $\delta\alpha/C_l'$, which is continuous and antisymmetrical about the centre-line of the model. In the corresponding symmetrical problem $\delta\alpha$ is split up into a uniform correction $\Delta\alpha$ to incidence and a residual upwash. Similarly it would be convenient to express most of the antisymmetrical $\delta\alpha$ as a linear twist proportional to y/s, which could be regarded as a uniform rate of roll, but this representation would be unrealistic unless the model were free to roll. Since $\delta\alpha$ is continuous, it would be unsatisfactory to interpret the tunnel interference as a correction to aileron setting and a residual upwash, so that in the case of deflected ailerons the effect of $\Delta\alpha$ must normally be calculated as a whole.

The treatment in Ref. 4 is based on lifting-line theory, which is unsatisfactory for wings of moderately low aspect ratio and inapplicable to swept wings. However a procedure of this kind must be devised if basic calculations by lifting-surface theory are not available. For this purpose the reader is referred to the simplified method illustrated at the end of Appendix II. The deficiencies of the lifting-line theory[8] (Multhopp, 1938) are partly taken into account by

(i) the device to include sweepback in section 5.2 of Ref. 2,

(ii) the rough formula (II 8) for the chordwise centre of pressure,

(iii) the modified formula (II 9) for C_l when $\alpha = y/s$.

δC_l is then calculated as that corresponding to an equivalent uniform rate of roll, *viz.*,

$$\delta\alpha = \left\{\frac{(\delta\alpha)_{3/4}}{y/s}\right\}_m \cdot \frac{y}{s} ,$$

where the quantity $\{(\delta\alpha)_{3/4}/(y/s)\}_m$ is estimated from equation (II 10). In the example considered, a fair degree of accuracy was obtained, but the simplified method of Appendix II is only suggested as a substitute for the lifting-surface method which follows.

It will be seen that Multhopp's[9] (1950) lifting-surface theory is particularly convenient. The calculated load distribution corresponding to unconstrained potential flow past the given plan-form with a given aileron setting will normally be different from the actual loading on the model. However, if the theoretical aileron setting is chosen to give the measured C_l', the calculated loading should approximate to the experimental loading, so that the tunnel interference can be estimated well within the desired accuracy. A solution by Ref. 9 with two chordwise terms determines just the information required in equation (7.1),

$$\gamma = \text{local } cC_L/4s$$

$$\mu = \text{local } cC_m/4s \text{ (about local quarter-chord)}$$

at chordwise sections $|t| = s \sin \dfrac{n\pi}{m+1}$ $[n = 1, 2, \ldots \tfrac{1}{2}(m-1)]$.

The distance of the chordwise centre of pressure from the leading edge $x = x_l(t)$ is expressed as a fraction $X_{\text{c.p.}}$ of the local chord $c(t)$, so that

$$\left.\begin{aligned} x_0 &= x_l + X_{\text{c.p.}}c \\ &= x_l + c\left(\tfrac{1}{4} - \frac{\mu}{\gamma}\right) \end{aligned}\right\} . \qquad (7.2)$$

Furthermore it is easy to evaluate $\delta\alpha$ at the $\tfrac{1}{2}(m-1)$ sections $y = s \sin \{\nu\pi/(m+1)\}$ in terms of the two integrands

$$\gamma\left\{P_0 - \frac{x_0}{h} P_1\right\} \text{ and } \gamma P_1 .$$

Thus $\delta\alpha$ is obtained for the values of x and y appropriate to a solution by Multhopp's method. A set of linear simultaneous equations then determines the quantities $\delta\gamma$ and $\delta\mu$ at sections $y = s \sin \{\nu\pi/(m+1)\}$; $\delta\gamma$ is integrated to give

$$\begin{aligned} \delta C_l &= \tfrac{1}{2}A \int_{-1}^{1} \delta\gamma \cdot \frac{y}{s}\, d\left(\frac{y}{s}\right) \\ &= \frac{\pi A}{2(m+1)} \sum_{1}^{\frac{1}{2}(m-1)} \delta\gamma_\nu \sin \frac{2\pi\nu}{m+1} . \end{aligned} \qquad (7.3)$$

Then the correction $\Delta C_l = -\delta C_l$ to be applied to the measured C_l' is given by

$$-\frac{\Delta C_l}{C_l'} = \frac{\displaystyle\sum_{1}^{\frac{1}{2}(m-1)} \delta\gamma_\nu \sin \frac{2\pi\nu}{m+1}}{\displaystyle\sum_{1}^{\frac{1}{2}(m-1)} \gamma_\nu \sin \frac{2\pi\nu}{m+1}} . \qquad (7.4)$$

It is envisaged that calculations of this kind will always be carried out for $m = 7$; and a worked example in Appendix II explains the procedure in 8 simple steps, which are shown in Tables A1 to 8 respectively:

(1) Interpolation: P_0 and P_1 for each (ν, n) from the general tables, *e.g.*, Tables 4 and 5. This is done once for all for a given span of wing.

(2) Evaluation of $X_{c.p.}$ and x_0 in equation (7.2) for each n from the known free-stream solution (γ_n, μ_n) corresponding to the particular aileron.

(3) Integration: I and J in equation (7.1) for each ν.

(4) Evaluation of $\delta\alpha_\nu'$, $\delta\alpha_\nu''$ at the appropriate pivotal points in equation (II 6).

(5) Setting out the basic equations for $\delta\gamma_\nu$ and $\delta\mu_\nu$. It is assumed that these are already prepared from equations (114) of Ref. 9.

(6) Evaluation of right-hand sides L_ν and M_ν from $\delta\alpha_\nu'$ and $\delta\alpha_\nu''$.

(7) Solution of linear simultaneous equations for $\delta\gamma_\nu$ and $\delta\mu_\nu$.

(8) Evaluation of $\Delta C_l/C_l'$ in equation (7.4).

The corresponding analysis for symmetrical loading follows the same pattern. The tunnel interference is supposed to be independent of the measured C_m' and is determined from values of γ/C_L' and x_0, calculated from Ref. 9 as functions of τ/σ. In equation (7.1), Q_0 and Q_1 take the place of P_0 and P_1. Equation (7.2) still holds except in the special case $y = 0$; for in the calculation of γ and μ there is a small displacement in the centre-line chord [Ref. 9, section 5.3 and Table 22], and x_l, c have to be modified accordingly. Similarly, at the section $y = 0$, some care is needed regarding the values of x for which $\delta\alpha$ is required. From the solutions for $\delta\gamma/C_L'$ and $\delta\mu C_L'$, $\delta C_L/C_L'$ and $\delta C_m/C_L'$ are obtained from equations (133) and (140) of Ref. 9. Corresponding theoretical values of $\partial C_L/\partial\alpha$ and $\partial C_m/\partial\alpha$ will already be known; and in terms of these values the interference corrections

$$\left.\begin{aligned} \Delta\alpha &= C_L' \frac{\delta C_L}{C_L'} \Big/ \frac{\partial C_L}{\partial\alpha} \\ \Delta C_m &= -\,C_L' \frac{\delta C_m}{C_L'} + \Delta\alpha \frac{\partial C_m}{\partial\alpha} \end{aligned}\right\} \qquad \ldots \quad (7.5)$$

are applied to the measured incidence and C_m' respectively. By the definition of $\Delta\alpha$ there is no interference correction to C_L', and the residual correction ΔC_m is independent of pitching axis.

When the rolling moment is measured on a half-model, the spanwise loading is symmetrical as in the preceding paragraph. By considering first of all a complete model in a tunnel of dimensions $2b \times h$, the tunnel-induced $\delta\alpha$ will be obtained from equation (7.1) when P_0 and P_1 $(\mu = h/b)$ are replaced by Q_0 and Q_1 $(\mu = h/2b)$. Equations (7.5) still apply; and this distributed upwash will also cause an incremental rolling moment given by

$$\delta C_l = A \int_0^1 \delta\gamma \frac{y}{s}\, d\left(\frac{y}{s}\right) \quad [\textit{cf.}\ \text{equation (7.3)}]$$

$$= \frac{\pi A}{8}\,[0\cdot0404\delta\gamma_0 + 0\cdot3440\delta\gamma_1 + 0\cdot5030\delta\gamma_2 + 0\cdot3525\,\delta\gamma_3]\,, \qquad \ldots \quad (7.6)$$

where $\delta\gamma_\nu$ is the value of $\delta\gamma$ when $y = s \sin \frac{1}{8}\nu\pi$ $(m = 7)$. Then, in addition to equations (7.5) the measured C_l' will require a residual correction

$$\Delta C_l = -\,C_L' \frac{\delta C_l}{C_L'} + \Delta\alpha \frac{\partial C_l}{\partial\alpha}\,, \qquad \ldots \quad (7.7)$$

where $\partial C_l/\partial\alpha$ is defined in the sense of equation (7.6). There may still remain an important factor to apply to $(C_l' + \Delta C_l)$, if outboard control surfaces are deflected and the practical condition of antisymmetrical ailerons is required. This determination of rolling power is not so much a problem of tunnel interference as of lifting-surface theory, and is best made by Ref. 9. A shorter approximate treatment, based on a modified lifting-line theory, is given in Ref. 2. If the aileron of a half-model is deflected through an angle ξ, the corrected rolling moment is†

$$C_l = (C_l' + \Delta C_l)\left(\frac{\partial C_l}{\partial \xi}\right)_a \Big/ \left(\frac{\partial C_l}{\partial \xi}\right)_s , \quad \ldots \quad (7.8)$$

where $(\partial C_l/\partial\xi)_a$ for antisymmetrical loading and $(\partial C_l/\partial\xi)_s$ for symmetrical loading are found independently.

When the spanwise loading on a complete model is asymmetrical, the tunnel interference on lift, rolling moment and pitching moment are obtained by writing

$$\begin{aligned} \gamma &= \gamma_a + \gamma_s \\ &= C_l' \frac{\gamma_a}{C_l'} + C_L' \frac{\gamma_s}{C_L'} , \end{aligned} \quad \ldots \quad (7.9)$$

and by considering the two parts quite separately in equations (7.4) and (7.5).

8. *Corrections to Drag and Yawing Moment.*—As regards the interference on C_D, C_c and C_n, the coefficients of drag, cross-wind force and yawing moment, there may be corrections to C_c and C_n due to tunnel-induced sidewash, but‡ these are beyond the scope of the present report. There will, however, be corrections to C_D and C_n due to induced drag. The effect of tunnel walls on yawing moment is considered on the basis of lifting-line theory in Ref. 3. A similar treatment will cater for a lifting line along the locus of the centres of pressure. This involves an assumption about the spanwise location of induced drag, and it is necessary to point out that the assumption is plausible, yet without rigorous justification.

Under tunnel conditions the total induced drag and induced yawing moment† on a wing are given by

$$\left.\begin{aligned} C_{Di}' &= -A\int_{-1}^{1} \gamma(\alpha_i + \delta\alpha)\, d(y/s) \\ C_{ni}' &= \tfrac{1}{2}A\int_{-1}^{1} \gamma(\alpha_i + \delta\alpha)(y/s)\, d(y/s) \end{aligned}\right\} , \quad \ldots \quad (8.1)$$

where

α_i, the induced incidence due to finite aspect ratio, plays no part in the tunnel interference,

$\delta\alpha$ is the tunnel-induced angle of upwash at the centre of pressure

and

γ is given in equation (7.9).

When $\delta\alpha = \delta\alpha_a + \delta\alpha_s$ is split into its antisymmetrical and symmetrical parts, the contributions due to tunnel interference from equation (8.1) are

$$\delta C_D = -A\int_{-1}^{1} (\gamma_a\,\delta\alpha_a + \gamma_s\,\delta\alpha_s)\, d(y/s) , \quad \ldots \quad (8.2)$$

$$\delta C_n = \tfrac{1}{2}A\int_{-1}^{1} (\gamma_a\,\delta\alpha_s + \gamma_s\,\delta\alpha_a)(y/s)\, d(y/s) , \quad \ldots \quad (8.3)$$

†As the axes used in Fig. 1 do not conform to the standard axes of an aircraft, the sign of the aileron setting ξ has been chosen to give the usual positive C_l/ξ. It should also be noted that the sign of C_{ni}' in equation (8.1) is consistent with the standard negative theoretical value of $C_{ni}/C_L C_l$.

‡This aspect of tunnel interference is considered by R. S. Swanson in A.R.C. Report 6969 (N.A.C.A. ARR February, 1943), entitled 'Jet-boundary corrections to a yawed model in a closed rectangular wind tunnel'.

where each $\delta\alpha_a$ and $\delta\alpha_s$ is calculated at the position of the chordwise centre of pressure corresponding to the particular γ_a or γ_s with which it is associated. Thus equation (7.1) gives

$$\text{for } \delta C_D, \quad \left.\begin{aligned} \delta\alpha_a &= I_a + J_a(x_0/h)_a \\ \delta\alpha_s &= I_s + J_s(x_0/h)_s \end{aligned}\right\} \qquad \ldots \qquad (8.4)$$

$$\text{and for } \delta C_n, \quad \left.\begin{aligned} \delta\alpha_a &= I_a + J_a(x_0/h)_s \\ \delta\alpha_s &= I_s + J_s(x_0/h)_a \end{aligned}\right\}, \qquad \ldots \qquad (8.5)$$

where from equation (7.2)

$$(x_0/h)_a = x_l/h + \frac{c}{h}\left(\tfrac{1}{4} - \frac{\mu_a}{\gamma_a}\right)$$

and $(x_0/h)_s$ is given similarly. When drag is considered, γ_a and γ_s are treated separately, but in the case of yawing moment there is no contribution δC_n unless both γ_a and γ_s exist, *i.e.*, the spanwise loading is asymmetrical. It is necessary to consider two conditions of asymmetrical loading

(i) when the wing is at uniform incidence and the ailerons are antisymmetrically deflected

(ii) when the wing is at zero incidence and the ailerons are asymmetrical.

Separate calculations of both $\delta\alpha_a$ and $\delta\alpha_s$ will be required in the two cases.

By the usual method of integration, as in equation (143) of Ref. 9, equation (8.2) becomes

$$\delta C_D = (\delta C_D)_a + (\delta C_D)_s\,, \qquad \ldots \qquad (8.6)$$

where

$$(\delta C_D)_a = -\frac{\pi A}{m+1}\sum_{-\frac{1}{2}(m-1)}^{\frac{1}{2}(m-1)} (\gamma_a)_\nu\,(\delta\alpha_a)_\nu \cos\frac{\nu\pi}{m+1} \text{ is proportional to } (C_l')^2,$$

$$(\delta C_D)_s = -\frac{\pi A}{m+1}\sum_{-\frac{1}{2}(m-1)}^{\frac{1}{2}(m-1)} (\gamma_s)_\nu\,(\delta\alpha_s)_\nu \cos\frac{\nu\pi}{m+1} \text{ is proportional to } (C_L')^2,$$

and $(\delta\alpha_a)_\nu$, $(\delta\alpha_s)_\nu$ are given in equation (8.4), when $y = s \sin\dfrac{\nu\pi}{m+1}$.

The measured drag consists of five parts

$$C_D' = C_{D0} + (C_D')_a + (\delta C_D)_a + (C_D')_s + (\delta C_D)_s\,, \qquad \ldots \qquad (8.7)$$

where C_{D0} is the profile drag. C_{Di}' in equation (8.1) is a theoretical estimate of the last four terms; and $(\delta C_D)_a$ and $(\delta C_D)_s$ are easily computed from equation (8.6). It is approximately true that $(C_D')_a$ is proportional to $(C_l')^2$ and that $(C_D')_s$ is proportional to $(C_L')^2$. C_l' requires a correction ΔC_l from equation (7.4), but by equation (7.5) there is no correction to C_L'. Thus the corrected experimental drag coefficient is

$$C_D = C_{D0} + \left(1 + \frac{\Delta C_l}{C_l'}\right)^2 (C_D')_a + (C_D')_s\,. \qquad \ldots \qquad (8.8)$$

From equations (8.7) and (8.8) the correction to be applied to C_D' is

$$\begin{aligned} \Delta C_D &= C_D - C_D' \\ &= \frac{\Delta C_l}{C_l'}\left(2 + \frac{\Delta C_l}{C_l'}\right)(C_D')_a - (\delta C_D)_a - (\delta C_D)_s \\ &= 2\frac{\Delta C_l}{C_l'}\{(C_D')_a + (\delta C_D)_a\} - (C_l')^2 \frac{(\delta C_D)_a}{(C_l')^2} - (C_L')^2 \cdot \frac{(\delta C_D)_s}{(C_L')^2} \\ &\quad + \text{(second-order terms)} . \qquad (8.9) \end{aligned}$$

The measured C_D' in equation (8.7) must be split into three parts

$$C_{D0}, \quad (C_D')_a + (\delta C_D)_a, \quad (C_D')_s + (\delta C_D)_s,$$

the second of which is required. Then from the calculated values of $\Delta C_l/C_l'$ in equation (7.4), $(\delta C_D)_a/(C_l')^2$ and $(\delta C_D)_s/(C_L')^2$ in equation (8.6), ΔC_D may be evaluated.

The effect of tunnel interference on yawing moment in equation (8.3) becomes

$$\delta C_n = \frac{\pi A}{2(m+1)} \sum_{1}^{\frac{1}{2}(m-1)} \{(\gamma_a)_\nu (\delta\alpha_s)_\nu + (\gamma_s)_\nu (\delta\alpha_a)_\nu\} \sin\frac{2\nu\pi}{m+1} , \qquad (8.10)$$

where $\delta\alpha_a$ and $\delta\alpha_s$ are given in equation (8.5). For a given wing with a pair of ailerons there are three types of loading

(*a*) symmetrical—uniform incidence (ailerons undeflected),
(*b*) symmetrical—ailerons deflected in the same sense ($\alpha = 0$),
(*c*) antisymmetrical—ailerons deflected in opposite senses.

In the absence of (*c*) the purely symmetrical loading gives $C_n = \delta C_n = 0$. (*a*) and (*c*) combine to give the asymmetrical loading (i) mentioned earlier ; (*b*) and (*c*) combine to give the loading (ii). Thus the measured yawing moment can be split into

$$C_n' = \{(C_n')_1 + (\delta C_n)_1\} + \{(C_n')_2 + (\delta C_n)_2\} , \qquad (8.11)$$

where the two parts correspond to loadings (i) and (ii). The measured C_l' is common to both, but there are respective contributions $(C_L')_1$ and $(C_L')_2$ to the measured lift coefficient. From equation (8.10)

$$\left.\begin{aligned} (\delta C_n)_1 &\text{ is proportional to } (C_L')_1 C_l' \\ (\delta C_n)_2 &\text{ is proportional to } (C_L')_2 C_l' \end{aligned}\right\} .$$

The corrected experimental yawing-moment coefficient is

$$C_n = \left(1 + \frac{\Delta C_l}{C_l'}\right)^2 \{(C_n')_1 + (C_n')_2\} . \qquad (8.12)$$

From equations (8.11) and (8.12) the correction to be applied to C_n' is

$$\Delta C_n = 2\frac{\Delta C_l}{C_l'} C_n' - (C_L')_1 C_l' \frac{(\delta C_n)_1}{(C_L')_1 C_l'} - (C_L')_2 C_l' \frac{(\delta C_n)_2}{(C_L')_2 C_l'} + \text{(second-order terms)}. \qquad (8.13)$$

Then from the calculated values of $\Delta C_l/C_l'$ in equation (7.4), $\delta C_n/C_L' C_l'$ for loadings (i) and (ii) in equation (8.10), ΔC_n may be evaluated.

9. *Results and Discussion.*—In section 7 and 8, for a complete wing with control surfaces the interference corrections due to the upwash induced by the tunnel walls were obtained as follows :

$$\left.\begin{aligned}
\Delta\alpha &= C_L' \frac{\Delta\alpha}{C_L'} \\
\Delta C_L &= 0 \\
\Delta C_l &= C_l' \frac{\Delta C_l}{C_l'} \\
\Delta C_m &= C_L' \frac{\Delta C_m}{C_L'} \\
\Delta C_D &= (C_D')_a \, . \, 2\frac{\Delta C_l}{C_l'} - (C_l')^2 \frac{(\delta C_D)_a}{(C_l')^2} - (C_L')^2 \frac{(\delta C_D)_s}{(C_L')^2} \\
\Delta C_c &= 0 \\
\Delta C_n &= C_n' \, . \, 2\frac{\Delta C_l}{C_l'} - (C_L')_1 C_l' \frac{(\delta C_n)_1}{(C_L')_1 C_l'} - (C_L')_2 C_l' \frac{(\delta C_n)_2}{(C_L')_2 C_l'}
\end{aligned}\right\} \quad \ldots \quad \ldots \quad (9.1)$$

where the experimental coefficients C_L', C_l', C_D', C_n' are corrected for tunnel blockage only,

$C_L' = (C_L')_1 + (C_L')_2$ is explained after equation (8.11)

$C_D' \simeq C_{D0} + (C_D')_a + (C_D')_s$ is explained in equation (8.7)

and the remaining quantities are determined theoretically†.

These corrections are required in the case of a complete model of the arrowhead Wing B, whose plan-form is illustrated and defined in Fig. 4. Six-component balance measurements have been carried out in the N.P.L. Duplex Wind Tunnel on this model with six different pairs of ailerons. For control chord ratios of both $E = 0 \cdot 2$ and $E = 0 \cdot 4$, there are three spans of aileron $0 \cdot 36s < y < s$, $0 \cdot 54s < y < s$, $0 \cdot 72s < y < s$, and the wing semi-span $s = 0 \cdot 295\,b$.

Full details of the calculations of $\Delta C_l/C_l'$ are set out in Appendix II and for each pair of ailerons the corrections reduce C_l' by about 2 per cent. In the symmetrical problem of uniform incidence $\Delta\alpha/C_L' = 0 \cdot 040$, so that the correction to α is about + 11 per cent. The corresponding corrections, $\Delta\alpha/C_L'$, when controls are deflected symmetrically, are rather less ; and the effective ratio

$$\frac{\delta C_L}{C_L'} = \frac{\partial C_L}{\partial\alpha}\frac{\Delta\alpha}{C_L'}$$

is of the order $6\frac{1}{2}$ per cent, which is over three times the ratio $\Delta C_l/C_l'$ when the controls are deflected antisymmetrically. Tabulated results will be found in Table 8a ; and from these Fig. 5 has been prepared. Curves of $\delta C_L/C_L'$ and $\delta C_l/C_l'$ against the position of the inboard end of the aileron y_a/s show

(i) that $\delta C_L/C_L'$ changes a good deal with span of aileron,

(ii) that results for $E = 0 \cdot 4$ are slightly higher than results for $E = 0 \cdot 2$.

The latter is a consequence of the more forward centres of pressure when $E = 0 \cdot 4$.

---

†In accordance with the footnote to equation (7.8), it should be noted that $(\delta C_n)/C_L'C_l'$ is positive.

The dotted curves in Fig. 5 give the ratios

$\delta C_l/C_l'$ for the rolling moment on one half of the wing when the loading is symmetrical,

$\delta C_L/C_L'$ for the lift on one half of the wing when the loading is antisymmetrical.

It may be seen that typical results are :

$$\left.\begin{array}{r} \text{symmetrical } \delta C_L/C_L' = 0\cdot 065 \\ \text{symmetrical } \delta C_l/C_l' = 0\cdot 046 \\ \text{antisymmetrical } \delta C_L/C_L' = 0\cdot 025 \\ \text{antisymmetrical } \delta C_l/C_l' = 0\cdot 021 \end{array}\right\} \qquad (9.2)$$

Thus the hybrid cases, dotted in Fig. 5, bridge the gap. This is probably a feature of oblong tunnels ($\mu < 1$). It will be noted in Table 6 that along the leading diagonal $\eta = \tau$, Q_0 falls quite sharply in the range $\eta < 0\cdot 20$, so that for a given symmetrical loading there will be a smaller correction to the rolling moment on the half-wing than to the lift. This is not so for a square tunnel, as may be seen by differencing the columns of Table 2 of Ref. 1.

The orders of magnitude of the symmetrical $\delta C_L/C_L'$ and the antisymmetrical $\delta C_l/C_l'$ in equation (9.2) will now be verified by considering a small model of the arrowhead wing in the Duplex Tunnel. For a very small elliptically loaded wing, it is easily shown from equation (7.1) that

$$\delta\alpha = I_s = \frac{8s^2}{hb}\int_0^1 \frac{2C_L'}{\pi A} Q_0 \sqrt{\{1 - (\tau/\sigma)^2\}}\, d(\tau/\sigma)$$

$$= \frac{4C_L'}{A}\frac{\sigma^2 Q_0}{\mu} ,$$

so that on substituting for Wing B, $A = 2\cdot 64$, $\partial C_L'/\partial\alpha = 2\cdot 732$, $Q_0 = 0\cdot 1368$ from Table 6, and $\mu = \frac{1}{2}$,

$$\frac{\delta\alpha}{\alpha} = \frac{\delta C_L}{C_L'} = 1\cdot 13\sigma^2 = 0\cdot 098, \text{ when } \sigma = 0\cdot 295 . \qquad (9.3)$$

For a very small antisymmetrically loaded wing, the limiting form of P_0 in equation (6.4) is

$$P_0(\eta, \tau) = -\frac{1}{16\mu} . 2\eta\tau\left(\frac{d^2\phi_0}{d\eta^2}\right)_{\eta=0} = 3\cdot 85\eta\tau, \text{ when } \mu = \tfrac{1}{2} .$$

Then

$$\delta\alpha = I_a = \frac{8s^2}{hb}\int_0^1 \frac{16C_l'}{\pi A}\{3\cdot 85\,\eta\tau\}\frac{\tau}{\sigma}\sqrt{\{1 - (\tau/\sigma)^2\}}\, d(\tau/\sigma) .$$

Hence

$$\frac{\delta\alpha}{\eta/\sigma} = \frac{8C_l'}{A}\frac{3\cdot 85\sigma^4}{\mu} ,$$

so that on substituting for Wing B, $A = 2\cdot 64$, $\mu = \frac{1}{2}$, it follows from Appendix II, equation (II 11) that

$$\delta C_l/C_l' = 0\cdot 225\frac{3\cdot 85\,\sigma^4}{0\cdot 165} = 5\cdot 25\sigma^4 = 0\cdot 040, \text{ when } \sigma = 0\cdot 295 . \qquad (9.4)$$

The equations (9.3) and (9.4) only apply to infinitesimal wings, but they serve to show that, for symmetrical loading, tunnel interference is of order $(s/b)^2$, while for antisymmetrical loading it is of order $(s/b)^4$. Moreover the ratio

$$\frac{\delta C_l/C_l'}{\delta C_L/C_L'} = 4\cdot6\ (s/b)^2 \qquad \ldots \qquad (9.5)$$

$$= 0\cdot40 \text{ for the model of Wing B}$$

compares with the ratio from equations (9.2)

$$\frac{\delta C_l/C_l'}{\delta C_L/C_L'} = \frac{0\cdot021}{0\cdot065} = 0\cdot32\,.$$

The allusion to a small wing provides a simple demonstration that the magnitude of antisymmetrical wall interference is usually much less than that of symmetrical interference. For a square tunnel ($\mu = 1$) for example, it is easily shown that, in place of equations (9.3), (9.4) and (9.5)

$$\left.\begin{aligned} \delta C_L/C_L' &= 0\cdot56\sigma^2 = 0\cdot049 \\ \delta C_l/C_l' &= 0\cdot77\sigma^4 = 0\cdot006 \\ \frac{\delta C_l/C_l'}{\delta C_L/C_L'} &= 1\cdot4(s/b)^2 = 0\cdot12 \end{aligned}\right\}, \qquad \ldots \qquad (9.6)$$

when the model of Wing B is considered in a tunnel of the same breadth but twice the height of the Duplex Tunnel. Equations (9.6) suggest that the interference on an antisymmetrically loaded wing in a square tunnel would be small compared with the ratio $\Delta C_l/C_l' = 0\cdot021$ in equation (9.2).

The results for ΔC_D and ΔC_n in equation (9.1) are more complicated, because both symmetrical and antisymmetrical loadings have to be taken into account. The measured C_L' and C_D' have to be subdivided in order to apply the corrections. In accordance with section 9, the four theoretical quantities involving δC_D and δC_n are evaluated in Table 8b for the particular model of Wing B in the N.P.L. Duplex Wind Tunnel.

The third term in the expression for ΔC_D in equation (9.1) is the most significant ; and from Table 8b

$$0\cdot022(C_L')^2 < -\,(C_L')^2\,\frac{(\delta C_D)_s}{C_L'^2} < 0\cdot0255(C_L')^2\,. \qquad \ldots \qquad (9.7)$$

By Multhopp's theory (Ref. 9) the induced drag on Wing B at uniform incidence is

$$C_{Di} = 0\cdot121 C_L^2\,,$$

so that the contribution to ΔC_D in (9.7) is equal to + 21 per cent of C_{Di}, which can be important.

For all practical purposes it is found in Table 8b that

$$\frac{(\delta C_n)_1}{(C_L')_1 C_l'} = \frac{(\delta C_n)_2}{(C_L')_2 C_l'} = 0\cdot0435 \qquad \ldots \qquad (9.8)$$

for each pair of ailerons. Since the first term in the expression for ΔC_n in equation (9.1) is comparatively small, it is accurate enough to use from Table 8a

$$\Delta C_l/C_l' = -\,0\cdot021.$$

With this value and equation (9.8), the expression in equation (9.1) simplifies to

$$\Delta C_n = -\,0\cdot042 C_n' - 0\cdot0435 C_L' C_l'. \qquad \ldots \qquad (9.9)$$

From experiment $C_n'/C_L'C_l'$ is of the order $-\,0\cdot1$ or $-\,0\cdot2$, so that the correction to C_n' may exceed + 25 per cent.

10. *Concluding Remarks.*—(*a*) The general procedure for computing the interference on a lifting surface in the central horizontal plane of a closed rectangular tunnel has been simplified. For a given shape of tunnel, only four basic quantities P_0, P_1, Q_0, Q_1 are required as functions of two variables (η, τ). In equations (6.4), (6.8), (6.5), (6.9), these are expressed exactly as rapidly convergent series in terms of four functions f_1, f_2, f_3, f_4 of a single variable, which are tabulated in Tables 1 to 3.

(*b*) It is a simple matter to tabulate P_0, P_1, Q_0, Q_1 for any rectangular shape, and values for a duplex tunnel are given in Tables 4 to 7.

(*c*) In section 7 the evaluation of tunnel interference is conveniently associated with Multhopp's lifting-surface theory. Any other lifting-surface theory could be used, but the worked example in Appendix II shows considerable economy in computation.

(*d*) The snags that may arise in some other procedures are considered at the end of Appendix II, where a fairly simple, but somewhat speculative, attempt is made to do without a lifting-surface theory.

(*e*) The calculated interference corrections for specific tests at N.P.L. are as follows (section 9) :

equivalent lift	$-$ 10·9 per cent to $-$ 5·6 per cent dependent on the symmetrical loading
rolling moment	$-$ 2·5 per cent to $-$1·9 per cent for different ailerons
total centre of pressure	a residual forward movement of $0 \cdot 009\bar{c}$
drag	a possible + 21 per cent
yawing moment	a possible + 25 per cent or more.

(*f*) A physical explanation of the differences in magnitude of the various percentage corrections is that

$$\delta C_D/C_{Di}' \text{ and } \delta C_n/C_{ni}' \text{ depend on the ratio } \frac{\text{tunnel-induced upwash}}{\text{wing-induced upwash}} ,$$

while

$$\delta C_L/C_L' \text{ depends on the ratio } \frac{\text{tunnel-induced upwash}}{\text{geometric incidence}} .$$

It is known that

$$\frac{\text{wing-induced upwash}}{\text{geometric incidence}} \simeq \frac{\text{wing-induced lift}}{\text{lift by strip theory}} = \frac{\partial C_L/\partial \alpha}{2\pi \cos \Lambda} - 1$$

$$= -\, 0 \cdot 38_5 \text{ for the present wing,}$$

so that percentage corrections to drag and yawing moment would be expected to have opposite sign to the equivalent percentage correction to lift and to have magnitude about 2·6 times as great.

(*g*) The smaller correction to rolling moment is explained in section 9 by allusion to a small model. It seems that, for a given ratio of wing span to tunnel breadth, the interference due to antisymmetrical loading would be markedly less in a square tunnel than in a duplex tunnel.

(*h*) As the corrections to drag and yawing moment are so large, it would appear to be essential to estimate these corrections despite the considerable labour of computation.

(*i*) Unless these corrections can be applied with confidence, there is reason to doubt the validity of tunnel measurements of C_D and C_n under these conditions. It is desirable to confirm results by means of tests in which the relative size of model to tunnel is varied.

11. *Acknowledgements*.—The authors wish to acknowledge the assistance of the Mathematics Division of the N.P.L. in the calculation of the functions in Tables 1 and. Miss J. Elliott of the Aerodynamics Division, N.P.L. assisted in the preparation of Tables 3 to 7. Most of the other numerical results given in this report were calculated by Miss E. Tingle of the Aerodynamics Division, N.P.L.

REFERENCES

No.	*Author*	*Title, etc.*
1	W. E. A. Acum	Corrections for symmetrical swept and tapered wings in rectangular wind tunnels. R. & M. 2777. April, 1950.
2	L. W. Bryant and H. C. Garner ..	Control testing in wind tunnels. R. & M. 2881. January, 1951.
3	D. J. Graham	Tunnel wall corrections to rolling and yawing moments due to aileron deflection in closed rectangular wind tunnel. N.A.C.A. A.R.R. 4F21. TIB 877. January, 1945.
4	J. Sanders and J. R. Pounder	Wall interference in wind tunnels of closed rectangular section. N.R.C. Canada Report AR-7. 1949. Supplement : N.R.C. Canada. Report AR-11. 1951.
5	H. Glauert	*The elements of aerofoil and airscrew theory*. 2nd edition. Cambridge University Press. 1948.
6	W. S. Brown	Wind tunnel corrections on ground effect. R. & M. 1865. July, 1938
7	F. W. J. Olver	Transformation of certain series occurring in aerodynamic interference calculations. *Quart. J. Mech. App. Math.*, Vol. II, Pt. 4, p. 452. 1949.
8	H. Multhopp	The calculation of the lift distribution of aerofoils. *L.F.F.* Vol. 15, No. 4. R.T.P. Translation No. 2392. A.R.C. 8516. 1938.
9	H. Multhopp	Methods for calculating the lift distribution of wings. (Subsonic lifting-surface theory.) R. & M. 2884, January, 1950.
10	G. N. Watson	*A treatise on the theory of Bessel functions*. 2nd edition. Cambridge University Press. 1948.

APPENDIX I

The Functions $f(\lambda)$ and $F(\lambda)$.—Consider the functions

$$f(\lambda) = \frac{1}{\lambda^2} + 2 \sum_{n=1}^{\infty} (-1)^n \frac{\lambda}{(\lambda^2 + n^2)^{3/2}}, \text{ when } \lambda > 0 .$$

$$= -f(|\lambda|), \text{ when } \lambda < 0 :$$

and

$$F(\lambda) = \frac{1}{2\lambda^2} + 2 \sum_{n=1}^{\infty} \frac{(-1)^n}{n^2} \frac{\lambda}{\sqrt{(\lambda^2 + n^2)}}, \text{ when } \lambda > 0,$$

$$= -F(|\lambda|), \text{ when } \lambda < 0.$$

By differentiating term by term it may be seen that $F'(\lambda) \equiv f(\lambda)/\lambda$. As $\lambda \to +\infty$, $f(\lambda) \to 0$, and $F(\lambda) \to -\pi^2/6$.

For small λ,

$$f(\lambda) = \frac{1}{\lambda^2} + 2\sum_{n=1}^{m}(-1)^n \frac{\lambda}{(\lambda^2+n^2)^{3/2}} + 2\sum_{n=m+1}^{\infty}(-1)^n \frac{\lambda}{(\lambda^2+n^2)^{3/2}}, \quad m \text{ being any integer}$$

$$= \frac{1}{\lambda^2} + 2\sum_{n=1}^{m}(-1)^n \frac{\lambda}{(\lambda^2+n^2)^{3/2}} + 2\lambda\left\{\sum_{n=m+1}^{\infty}\frac{(-1)^n}{n^3} - \frac{3}{2}\lambda^2\sum_{n=m+1}^{\infty}\frac{(-1)^n}{n^5} + \ldots\right\},$$

but this equation is useless for computing $f(\lambda)$ for large λ.

However, if λ is large, a more convenient expression for $f(\lambda)$ is obtained by considering the function

$$\chi(Z) = \frac{1}{(\lambda^2+Z^2)^{1/2}\sin\pi Z} = \frac{1}{\sin\pi Z}\,\frac{1}{|(\lambda^2+Z^2)|^{1/2}}\exp\left\{\frac{-i}{2}\left[\arg(Z-i\lambda) + \arg(Z+i\lambda)\right]\right\},$$

where $Z = X + iY$. This function has poles at the points $Z = 0, \pm 1, \pm 2 \ldots$.

When the integral of $\chi(Z)$ is taken round the contour shown in Fig. 3 and the limit as the small circles shrink to the points $Z = \pm i\lambda$ is considered as $n \to \infty$ it follows that

$$\frac{1}{\lambda} + 2\sum_{n=1}^{\infty}\frac{(-1)^n}{\sqrt{(\lambda^2+n^2)}} = 2\int_1^{\infty}\frac{dt}{\sinh\pi\lambda t\,\sqrt{(t^2-1)}}$$

$$= 4\int_1^{\infty}\{e^{-\pi\lambda t} + e^{-3\pi\lambda t} + \ldots\}\frac{dt}{\sqrt{(t^2-1)}}$$

$$= 4\{K_0(\pi\lambda) + K_0(3\pi\lambda) + K_0(5\pi\lambda) + \ldots\}.$$

Hence, differentiating,

$$f(\lambda) = \frac{1}{\lambda^2} + 2\sum_{n=1}^{\infty}\frac{(-1)^n\lambda}{(\lambda^2+n^2)^{3/2}} = 4\pi\{K_1(\pi\lambda) + 3K_1(3\pi\lambda) + 5K_1(5\pi\lambda) + \ldots\},$$

which is a rapidly converging series unless λ is small.

For the purposes of computing tunnel interference the quantities required are

$$f'(\lambda) + F'(\lambda) = f'(\lambda) + f(\lambda)/\lambda \quad\text{and}\quad f'(\lambda) + f(\lambda)/\lambda + 1/\lambda^3,$$

i.e., $f_3(\lambda)$ and $f_4(\lambda)$ respectively.

These functions have been calculated in the Mathematics Division of the N.P.L. and the values of $f_3(\lambda)$ and $f_4(\lambda)$ for positive values of λ are given in Table 2. Since $f(\lambda)$ is an odd function of λ, $f_3(\lambda)$ and $f_4(\lambda)$ are both even functions of λ. The values given in Table 2 may contain errors of up to 3 or 4 in the sixth decimal when $\lambda < 0{\cdot}4$, but otherwise they are accurate to within 2 in the sixth decimal. Table 3 has been prepared to facilitate interpolation in the values of $f_4(\lambda)$, so that second differences, will give values with an error of not more than one in the fourth decimal place. This accuracy should be ample for the purpose of calculating tunnel interference. When $f_4(\lambda)$ is known $f_3(\lambda)$ is obtained by subtracting $1/\lambda^3$. For values of $\lambda > 2$, interpolation in Table 2 using second differences should give the same accuracy.

APPENDIX II

Worked Example.—To illustrate the methods of calculation, the interference on a complete model of the arrowhead Wing B with deflected ailerons in the N.P.L. Duplex Wind Tunnel is evaluated in detail by the lifting-surface method and by a simplified method.

Wing B has aspect ratio $A = 2 \cdot 64$, taper ratio $\lambda = 7/18$ and angle of sweepback $\Lambda = 45$ deg at the quarter-chord. The origin of co-ordinates is chosen to be the leading apex of the wing, so that

$$\left.\begin{aligned} &\text{the leading edge is} \quad x_l(t) = \tfrac{7}{6}t = \tfrac{7}{6}s\cos\theta \\ &\text{the trailing edge is} \quad x_t(t) = c_0 + \tfrac{1}{2}t = c_0 + \tfrac{1}{2}s\cos\theta \\ &\text{and the chord is} \quad c = \bar{c}(1 \cdot 44 - 0 \cdot 88y/s) \end{aligned}\right\} , \quad \ldots \quad \ldots \quad \ldots \quad \text{(II 1)}$$

where $s = 4 \cdot 125$ ft, $c_0 = 4 \cdot 5$ ft, $\bar{c} = 3 \cdot 125$ ft. The Duplex Wind Tunnel is of breadth $b = 14$ ft, and of height $h = 7$ ft.

Lifting-Surface Method.—When the load distribution on the plan-form has been calculated by Multhopp's lifting-surface theory (Ref. 9) with two chordwise terms, this is found to be the most convenient starting point for evaluating tunnel interference. There is then no need to guess the local chordwise centres of pressure; and the tunnel-induced angle of upwash is readily converted into an incremental load distribution. The antisymmetrical wing loading due to deflected ailerons, computed by means of Ref. 9, determines the non-dimensional circulation

$$\gamma = \Gamma/2sV$$

and the chordwise centre of pressure

$$X_{\text{c.p.}} = \tfrac{1}{4} - \frac{\mu}{\gamma}$$

at spanwise stations $t = s\sin\{n\pi/(m+1)\}(m = 7 : n = 1, 2, 3)$. The loading is represented by a vortex of strength Γ situated along the locus of the chordwise centre of pressure

$$x = x_0 = x_l + X_{\text{c.p.}}(x_t - x_l) = \tfrac{7}{6}t + X_{\text{c.p.}}(c_0 - \tfrac{2}{3}t)$$

and the associated trailing vortex sheet. Then in the Duplex Wind Tunnel

$$x_0/h = \tfrac{7}{3}\tau + X_{\text{c.p.}}(\tfrac{9}{14} - \tfrac{4}{3}\tau) \quad \ldots \quad \ldots \quad \ldots \quad \ldots \quad \ldots \quad \ldots \quad \ldots \quad \text{(II 2)}$$

is known when

$$\tau = \tau_n = t_n/b = \sigma\sin\frac{n\pi}{8} \quad (n = 1, 2, 3) ,$$

where

$$\sigma = s/b = 0 \cdot 29464.$$

It is implicitly assumed that these values of x_0/h are close enough to the uncorrected experimental conditions. The uncorrected experimental spanwise loading is supposed to be proportional to the calculated values γ_1, γ_2 and γ_3 at the respective stations $y = 0 \cdot 3827s$, $0 \cdot 7071s$ and $0 \cdot 9239s$. The corresponding coefficient of rolling moment is

$$\begin{aligned} C_l &= \frac{\pi A}{16}(0 \cdot 7071\gamma_1 + \gamma_2 + 0 \cdot 7071\gamma_3) \\ &= 0 \cdot 3665\gamma_1 + 0 \cdot 5184\gamma_2 + 0 \cdot 3665\gamma_3 \quad \ldots \quad \ldots \quad \ldots \quad \ldots \quad \ldots \quad \text{(II 3)} \end{aligned}$$

for the particular Wing B. The calculated tunnel interference will therefore be multiplied by the factor

$$C_l'/(0\cdot 3665\gamma_1 + 0\cdot 5184\gamma_2 + 0\cdot 3665\gamma_3),$$

where C_l' is the uncorrected experimental coefficient.

From equation (7.1), tunnel interference amounts to a distributed angle of upwash

$$w/V = \frac{8s^2}{bh}\left(\int_0^1 \gamma(P_0 - P_1 x_0/h)\,d(\tau/\sigma) + \frac{x}{h}\int_0^1 \gamma P_1\,d(\tau/\sigma)\right), \qquad \text{(II 4)}$$

where γ stands for the uncorrected experimental spanwise loading, x_0/h is given in equation (II 2) and the parameters P_0 and P_1 are tabulated in Tables 4 and 5. The two integrals in equation (II 4) are evaluated separately. On writing the integrand as a Fourier series

$$\sum_{p=1}^{3} a_{2p} \sin 2p\theta\ ,$$

it may be shown that

$$\frac{8s^2}{bh}\int_0^1 W_n\,d(\tau/\sigma) = \frac{8s^2}{bh}\,\frac{\pi}{16}\,(2\cdot 1879W_1 + 1\cdot 2610W_2 + 0\cdot 8301W_3)$$

$$= (0\cdot 5967W_1 + 0\cdot 3439W_2 + 0\cdot 2264W_3)\ . \qquad \text{(II 5)}$$

w/V is calculated at the pivotal points required for a solution ($m = 7$) by Multhopp's theory. Three spanwise stations are involved

$$\eta = \eta_\nu = \sigma \sin\frac{\nu\pi}{8} = 0\cdot 29464 \sin\frac{\nu\pi}{8} \qquad (\nu = 1, 2, 3)\ .$$

At each of these stations, w/V is required at two chordwise positions $0\cdot 9045c$ and $0\cdot 3455c$, where respectively

$$\left.\begin{aligned} x/h = x'/h &= 0\cdot 58146 + 0\cdot 33216 \sin\frac{\nu\pi}{8} \\ x/h = x''/h &= 0\cdot 22211 + 0\cdot 55177 \sin\frac{\nu\pi}{8} \end{aligned}\right\} \qquad \text{(II 6)}$$

These six values of w/V are sufficient to determine an antisymmetrical solution on the basis of equations (114) and (115) of Ref. 9 with $m = 7$.

Having formulated the problem, the first step is to use Tables 4 and 5 to obtain by interpolation the values of P_0 and P_1 when $\tau = \tau_n$ and $\eta = \eta_\nu$ $(n, \nu = 1, 2, 3)$:

TABLE A 1

Values of P_0

n	τ_n	η_ν		
		0·11275	0·20834	0·27221
1	0·11275	0·03688	0·05171	0·05357
2	0·20834	0·05171	0·08177	0·09328
3	0·27221	0·05357	0·09328	0·11551

TABLE A 1—*continued.*

Values of P_1

n	τ_n	η_ν		
		0·11275	0·20834	0·27221
1	0·11275	0·07076	0·09514	0·09465
2	0·20834	0·09514	0·14730	0·16427
3	0·27221	0·09465	0·16427	0·20239

It will be noted that τ and η are interchangeable in both tables.

The second step is to copy γ and $X_{c.p.}$ from Multhopp's theory and to evaluate x_0/h from equation (II 2) for each antisymmetrical loading. For the present calculations three spans and two chords of aileron were considered.

TABLE A 2

Aileron span	$0 \cdot \dot{3}\dot{6}s < y < s$		$0 \cdot \dot{5}\dot{4}s < y < s$		$0 \cdot \dot{7}\dot{2}s < y < s$	
Chord ratio	$E = 0 \cdot 2$	$E = 0 \cdot 4$	$E = 0 \cdot 2$	$E = 0 \cdot 4$	$E = 0 \cdot 2$	$E = 0 \cdot 4$
γ_1	0·12626	0·16666	0·03539	0·05171	0·00900	0·01417
γ_2	0·19952	0·25782	0·15999	0·20700	0·06677	0·08936
γ_3	0·13723	0·17398	0·12380	0·15654	0·10143	0·12742
$(X_{c.p.})_1$	0·6952	0·5748	0·6710	0·5863	0·6322	0·5796
$(X_{c.p.})_2$	0·5952	0·4878	0·6425	0·5227	0·6809	0·5588
$(X_{c.p.})_3$	0·5291	0·4235	0·5616	0·4473	0·6201	0·4908
$(x_0/h)_1$	0·6055	0·5462	0·5936	0·5518	0·5745	0·5485
$(x_0/h)_2$	0·7034	0·6642	0·7207	0·6769	0·7347	0·6901
$(x_0/h)_3$	0·7833	0·7537	0·7924	0·7604	0·8087	0·7725

The third step is to evaluate the integrals in equation (II 4) from equation (II 5). Details are set out here for the particular aileron of chord ratio $E = 0 \cdot 2$ and span $0 \cdot \dot{5}\dot{4}s < y < s$:

TABLE A 3

Values of W	ν	n			$\frac{8s^2}{bh}\int_0^1 W\, d(\tau/\sigma)$
		1	2	3	
$\gamma_n(P_0 - (x_0/h)_n P_1)$	1	$-0 \cdot 00018$	$-0 \cdot 00270$	$-0 \cdot 00265$	$-0 \cdot 00164 = I_1$
$\gamma_n P_1$	1	0·00250	0·01522	0·01172	$0 \cdot 00938 = J_1$
$\gamma_n(P_0 - (x_0/h)_n P_1)$	2	$-0 \cdot 00017$	$-0 \cdot 00390$	$-0 \cdot 00457$	$-0 \cdot 00248 = I_2$
$\gamma_n P_1$	2	0·00337	0·02357	0·02034	$0 \cdot 01472 = J_2$
$\gamma_n(P_0 - (x_0/h)_n P_1)$	3	$-0 \cdot 00009$	$-0 \cdot 00402$	$-0 \cdot 00555$	$-0 \cdot 00269 = I_3$
$\gamma_n P_1$	3	0·00335	0·02628	0·02506	$0 \cdot 01671 = J_3$
Integration factor		0·5967	0·3439	0·2264	

The fourth step is to obtain $\delta\alpha = w/V$ at the six points specified in equation (II 6)

TABLE A 4

ν	y/s	x_ν'/h	x_ν''/h	$\delta\alpha_\nu'$	$\delta\alpha_\nu''$	$(\delta\alpha_\nu)_{3/4}$†
1	0·3827	0·7086	0·4333	0·00501	0·00242	0·00429
2	0·7071	0·8164	0·6123	0·00954	0·00653	0·00871
3	0·9239	0·8884	0·7319	0·01215	0·00954	0·01143

The fifth step is to copy the equations (114) of Ref. 9 ($m = 7$), which are already available for Wing B :

TABLE A 5

$$
\begin{array}{rrrrrrl}
\gamma_1 & -0{\cdot}2547\gamma_2 & & & -0{\cdot}2394\mu_2 & & = L_1 \\
-0{\cdot}3343\gamma_1 & +\gamma_2 & -0{\cdot}2622\gamma_3 & -0{\cdot}0709\mu_1 & & -0{\cdot}2319\mu_3 & = L_2 \\
 & -0{\cdot}3352\gamma_2 & +\gamma_3 & & -0{\cdot}0606\mu_2 & & = L_3 \\
 & +0{\cdot}0608\gamma_2 & & +\mu_1 & +0{\cdot}0192\mu_2 & & = M_1 \\
-0{\cdot}0225\gamma_1 & & +0{\cdot}0583\gamma_3 & -0{\cdot}0896\mu_1 & +\mu_2 & +0{\cdot}0057\mu_3 & = M_2 \\
 & -0{\cdot}0270\gamma_2 & & & -0{\cdot}1142\mu_2 & +\mu_3 & = M_3
\end{array}
$$

where the right-hand sides

$$
\begin{aligned}
L_\nu &= a_{\nu\nu}[l_\nu'(\delta\alpha_\nu') - l_\nu''(\delta\alpha_\nu'')], \\
M_\nu &= a_{\nu\nu}[m_\nu''(\delta\alpha_\nu'') - m_\nu'(\delta\alpha_\nu')] .
\end{aligned}
$$

The quantities $a_{\nu\nu}$, l_ν', l_ν'', m_ν'', m_ν' are already available, and the sixth step is to compute the right-hand sides L_ν and M_ν :

TABLE A 6

ν	$a_{\nu\nu}$	l_ν'	l_ν''	m_ν''	m_ν'	L_ν	M_ν
1	0·4619	0·4637	−0·0333	0·2470	0·1838	0·00111	−0·00015
2	0·3536	0·4597	−0·0370	0·2426	0·1810	0·00164	−0·00005
3	0·1913	0·4955	−0·0018	0·2827	0·2062	0·00116	0·00004

The seventh step is the solution of the six equations in Table A 5 with the right-hand sides from Table A 6, which determine

TABLE A 7

$$
\begin{aligned}
\delta\gamma_1 &= 0{\cdot}00178, & \delta\mu_1 &= -0{\cdot}00032, \\
\delta\gamma_2 &= 0{\cdot}00278, & \delta\mu_2 &= -0{\cdot}00016, \\
\delta\gamma_3 &= 0{\cdot}00208, & \delta\mu_3 &= 0{\cdot}00010.
\end{aligned}
$$

Hence from equation (II 3), the corresponding tunnel-induced coefficient of rolling moment is $\delta C_l = 0{\cdot}00286$. The assumed spanwise loading in Table A 2 gives $C_l = 0{\cdot}1413$. Therefore the correction to be applied to the measured C_l' is

$$(\Delta C_l) = -\frac{0{\cdot}00286}{0{\cdot}1413}\, C_l' = -\, 0{\cdot}0202\, C_l' .$$

† In Table A4, $(\delta a_\nu)_{3/4}$ denotes the values of w/V at three-quarter chord which are only required for comparison with the simplified method.

The calculated interference for the different ailerons is as follows :

TABLE A 8

Aileron span	$0 \cdot \dot{3}\dot{6}s < y < s$		$0 \cdot \dot{5}\dot{4}s < y < s$		$0 \cdot \dot{7}\dot{2}s < y < s$	
Chord ratio	$E = 0 \cdot 2$	$E = 0 \cdot 4$	$E = 0 \cdot 2$	$E = 0 \cdot 4$	$E = 0 \cdot 2$	$E = 0 \cdot 4$
$\delta\gamma_1$	0·00294	0·00412	0·00178	0·00252	0·00086	0·00123
$\delta\gamma_2$	0·00446	0·00619	0·00278	0·00388	0·00137	0·00193
$\delta\gamma_3$	0·00327	0·00450	0·00208	0·00288	0·00104	0·00146
δC_l	0·00459	0·00637	0·00286	0·00399	0·00141	0·00197
C_l	0·2000	0·2585	0·1413	0·1836	0·0751	0·0982
$-(\Delta C_l)/C_{l'}$	0·0230	0·0246	0·0202	0·0217	0·0188	0·0201

Provided that preliminary free-stream calculations for the plan-form, *i.e.*, Table A 5 and most of Tables A 2 and A 6, have been obtained by Multhopp's theory (Ref. 9), the amount of additional work in the evaluation of tunnel interference outlined above is comparatively small. In the absence of these calculations, antisymmetric interference corrections can probably be estimated to sufficient accuracy by the following simplified method.

Simplified Method.—A two-dimensional lift slope $2\pi \cos \Lambda'$ is chosen in accordance with Ref. 2 (section 5.1 and equation (44)), such that

$$\tan \Lambda' = \left(1 - \frac{0 \cdot 8}{A(1 + \lambda)}\right) \tan \Lambda = 0 \cdot 7818 \,, \qquad \text{(II 7)}$$

i.e.,

$$\cos \Lambda' = 0 \cdot 7878 \text{ for Wing B.}$$

Multhopp's lifting-line theory (Ref. 8) is then used with

$$a_1 = 2\pi \cos \Lambda' = 4 \cdot 950$$

and the two-dimensional ratio $a_2/a_1 = 0 \cdot 5498$ for $E = 0 \cdot 2$. The particular antisymmetrical solution for a deflected aileron of span $0 \cdot \dot{5}\dot{4}s < y < s$ determines in place of the values in Table A 2

$$\gamma_1 = 0 \cdot 04560, \gamma_2 = 0 \cdot 17637, \gamma_3 = 0 \cdot 12502,$$

for which equation (II 3) gives $C_l = 0 \cdot 1540$. In order to compute tunnel interference it is necessary to guess values of $X_{\text{c.p.}}$, which cannot be deduced from experimental balance measurements. The best general method that can be suggested here is to assume that at all sections

$$X_{\text{c.p.}} = l_2 + \frac{3 \cdot 5(1 + 3\lambda)}{A(2 + 2\lambda) + 3 \cdot 5(1 + 3\lambda)} \left(1 - E + \frac{E(1 - \lambda)(2\pi - 4)}{3\pi - 4 + 4\lambda} - l_2\right), \qquad \text{(II 8)}$$

where l_2, the value from Glauert's two-dimensional hinged plate theory, is given in Ref. 2, equation (8). The quantity

$$1 - E + \frac{E(1 - \lambda)(2\pi - 4)}{3\pi - 4 + 4\lambda}$$

is the chordwise centre of pressure determined for a full-span control on a cropped delta wing by R. T. Jones' slow-aspect-ratio theory. The interpolation factor

$$\frac{3 \cdot 5(1 + 3\lambda)}{A(2 + 2\lambda) + 3 \cdot 5(1 + 3\lambda)}$$

is based on Multhopp's lifting-surface theory for antisymmetrical loading, and apparently changes little with sweepback and the dimensions of the aileron. The value of $X_{c.p.}$ from equation (II 8) may be $\pm 0\cdot03$ different from its best mean value, but this is not significant in the determination of tunnel interference. In the present example, $A = 2\cdot64$, $\lambda = 7/18$, $E = 0\cdot2$. Hence

$$X_{c.p.} = 0\cdot4353 + 0\cdot508\,(0\cdot8400 - 0\cdot4353)$$
$$= 0\cdot641 \text{ (for } n = 1, 2, \text{ and } 3).$$

When the calculations of Tables A 2, A 3 and A 4 are repeated with these values of γ and $X_{c.p.}$, the tunnel-induced angle of upwash at three-quarter chord is obtained:

TABLE A 9

ν	y/s	$\frac{8s^2}{bh}\int_0^1 W\,d(\tau/\sigma)$ for $W =$		$\frac{(x_\nu)_{3/4}}{h}$	$(\delta\alpha_\nu)_{3/4}$
		$\gamma_n[P_0 - (x_0/h)_n P_1]$	γP_1		
1	0·3827	−0·00180	0·01038	0·6325	0·00477
2	0·7071	−0·00271	0·01617	0·7599	0·00958
3	0·9239	−0·00295	0·01827	0·8451	0·01249

Now a simple procedure is needed to evaluate δC_l. The most convenient method is to use the modified lifting-line theory with $a_1 = 4\cdot950$ to estimate the rolling moment due to an antisymmetrical incidence $\alpha = y/s$. This is readily achieved from the equations of Table 4b of Ref. 8 using†

$$\left.\begin{aligned} &\text{'}\,b/c_\nu t_\nu\,\text{'} \equiv 4s/a_1 c_\nu = 0\cdot8081 s/c_\nu : \\ &3\cdot1317\gamma_1 - 0\cdot7654\gamma_2 = \alpha_1 = 0\cdot3827 \\ &-\gamma_1 + 4\cdot1328\gamma_2 - \gamma_3 = \alpha_2 = 0\cdot7071 \\ &-1\cdot8477\gamma_2 + 6\cdot9275\gamma_3 = \alpha_3 = 0\cdot9239 \end{aligned}\right\},$$

whence $\gamma_1 = 0\cdot1872$, $\gamma_2 = 0\cdot2658$, $\gamma_3 = 0\cdot2043$ and from equation (II 3), $(C_l)_{l.l.} = 0\cdot2813$. Some correction to this value is necessary to allow for the deficiencies of the lifting-line theory. The recommended formula is

$$C_l = 1\cdot15\,(C_l)_{l.l.} - 0\cdot15\,(C_l)_{s.t.}\,, \qquad \text{(II 9)}$$

where the factors $1\cdot15$ and $0\cdot15$ are roughly independent of plan-form and $(C_l)_{s.t.}$ is obtained on the basis of two-dimensional strip theory, *viz.*,

$$(C_l)_{s.t.} = 2\pi\cos\Lambda' \int_0^1 \alpha\,(y/s)\,(c/2\bar{c})\,d(y/s)$$
$$= 4\cdot950 \int_0^1 (y/s)^2\,(0\cdot72 - 0\cdot44\,y/s)\,d(y/s)$$
$$= 4\cdot950 \times 0\cdot13 = 0\cdot6435.$$

Hence

$$C_l = 1\cdot15 \times 0\cdot2813 - 0\cdot15 \times 0\cdot6435$$
$$= 0\cdot225.$$

†It should be noted that the suffix ν is different in Ref. 8 and Ref. 9. The definitions here (equation II 2) correspond to Ref. 9.

TABLE 1

Functions $f_1(\lambda), f_2(\lambda)$ for Evaluating P_0, Q_0

λ	$-f_1(\lambda)$	$f_2(\lambda)$	λ	$-f_1(\lambda)$	$f_2(\lambda)$
0·00	∞	−0·523599	2·00	0·011734	+0·067844
0·05	127·843051	0·519097	2·05	0·010028	0·065715
0·10	32·336810	0·505821	2·10	0·008570	0·063609
0·15	14·631548	0·484442	2·15	0·007324	0·061537
0·20	8·413747	0·456000	2·20	0·006260	0·059507
0·25	5·514765	−0·421807	2·25	0·005350	+0·057526
0·30	3·920105	3·383328	2·30	0·004572	0·055600
0·35	2·940517	0·342069	2·35	0·003907	0·053731
0·40	2·288904	0·299467	2·40	0·003339	0·051923
0·45	1·828717	0·256817	2·45	0·002854	0·050176
0·50	1·488454	−0·215214	2·50	0·002439	+0·048490
0·55	1·227797	0·175533	2·60	0·001782	0·045306
0·60	1·022614	0·138420	2·70	0·001301	0·042363
0·65	0·857705	0·104309	2·80	0·000950	0·039650
0·70	0·723060	0·073448	2·90	0·000694	0·037155
0·75	0·611814	−0·045930	3·00	0·000507	+0·034861
0·80	0·519083	0·021724	3·10	0·000370	0·032752
0·85	0·441275	−0·000707	3·20	0·000271	0·030814
0·90	0·375668	+0·017307	3·30	0·000198	0·029032
0·95	0·320151	0·032547	3·40	0·000144	0·027391
1·00	0·273047	+0·045263	3·50	0·000105	+0·025879
1·05	0·233003	0·055713	3·60	0·000077	0·024484
1·10	0·198913	0·064153	3·70	0·000056	0·023195
1·15	0·169862	0·070826	3·80	0·000041	0·022003
1·20	0·145084	0·075964	3·90	0·000030	0·020898
1·25	0·123941	+0·079777	4·00	0·000022	+0·019872
1·30	0·105891	0·082458	4·10	0·000016	0·018920
1·35	0·090478	0·084178	4·20	0·000012	0·018033
1·40	0·077313	0·085090	4·30	0·000009	0·017207
1·45	0·066066	0·085330	4·40	0·000006	0·016435
1·50	0·056457	+0·085014	4·50	0·000005	+0·015714
1·55	0·048247	0·084244	4·60	0·000003	0·015040
1·60	0·041232	0·083108	4·70	0·000002	0·014407
1·65	0·035237	0·081681	4·80	0·000002	0·013814
1·70	0·030114	0·080028	4·90	0·000001	0·013256
1·75	0·025736	+0·078202	5·00	0·000001	+0·012731
1·80	0·021995	0·076249	5·10	0·000001	0·012237
1·85	0·018797	0·074208	5·20	0·000001	0·011771
1·90	0·016065	0·072110			
1·95	0·013729	0·069981			

$$f_2(\lambda) = \frac{1}{\pi\lambda^2} \text{ for } \lambda > 5{\cdot}2$$

TABLE 2

Functions $f_3(\lambda), f_4(\lambda)$ for Evaluating P_1, Q_1

λ	$f_3(\lambda)$	$f_4(\lambda)$	λ	$f_3(\lambda)$	$f_4(\lambda)$
0·00	$-\infty$	−3·606171	2·00	−0·036186	+0·088814
0·05	8003·577147	3·577147	2·05	0·030559	0·085516
0·10	1003·491715	3·491715	2·10	0·025814	0·082166
0·15	299·650915	3·354619	2·15	0·021812	0·078808
0·20	128·173170	3·173170	2·20	0·018435	0·075479
0·25	−66·956485	−2·956485	2·25	−0·015585	
0·30	39·751635	2·714598	2·30	0·013178	
0·35	25·781221	2·457606	2·35	0·011146	
0·40	17·819928	2·194928	2·40	0·009429	
0·45	12·908721	1·934784	2·45	0·007978	
0·50	−9·683870	−1·683870	2·50	−0·006752	
0·55	7·457769	1·447251	2·60	0·004838	
0·60	5·858043	1·228413	2·70	0·003470	
0·65	4·670753	1·029424	2·80	0·002490	
0·70	3·766619	0·851167	2·90	0·001788	
0·75	−3·063956	−0·693585	3·00	−0·001284	
0·80	2·509057	0·555932	3·10	0·000923	
0·85	2·065316	0·436983	3·20	0·000664	
0·90	1·706963	0·335221	3·30	0·000478	
0·95	1·415333	0·248982	3·40	0·000344	
1·00	−1·176562	−0·176562	3·50	−0·000248	
1·05	0·980130	−0·116292	3·60	0·000178	
1·10	0·817912	−0·066597	3·70	0·000129	
1·15	0·683535	−0·026019	3·80	0·000093	
1·20	0·571942	+0·006762	3·90	0·000067	
1·25	−0·479077	+0·032923	4·00	−0·000048	
1·30	0·401664	0·053502	4·10	0·000035	
1·35	0·337037	0·069405	4·20	0·000025	
1·40	0·283016	0·081415	4·30	0·000018	
1·45	0·237811	0·090206	4·40	0·000013	
1·50	−0·199947	+0·096349	4·50	−0·000010	
1·55	0·168205	0·100332	4·60	0·000007	
1·60	0·141574	0·102567	4·70	0·000005	
1·65	0·119216	0·103396	4·80	0·000004	
1·70	0·100432	0·103110	4·90	0·000003	
1·75	−0·084644	+0·101945	5·00	−0·000002	
1·80	0·071365	0·100103	5·10	0·000001	
1·85	0·060191	0·097746	5·20	0·000001	
1·90	0·050784	0·095010	5·30	0·000001	
1·95	0·042861	0·092003	5·40	0·000001	

TABLE 3

Values of $f_4(\lambda)$

$\lambda = 0(0{\cdot}025)2{\cdot}100$

λ	$f_4(\lambda)$	λ	$f_4(\lambda)$	λ	$f_4(\lambda)$
0	−3·606 171	0·700	−0·851 167	1·400	+0·081 415
0·025	3·598 889	0·725	0·769 825	1·425	0·086 175
0·050	3·577 147	0·750	0·693 585	1·450	0·090 206
0·075	3·541 253	0·775	0·622 335	1·475	0·093 576
0·100	3·491 715	0·800	0·555 932	1·500	0·096 349
0·125	3·429 220	0·825	0·494 209	1·525	0·098 583
0·150	3·354 619	0·850	0·436 983	1·550	0·100 332
0·175	3·268 901	0·875	0·384 056	1·575	0·101 645
0·200	3·173 170	0·900	0·335 221	1·600	0·102 567
0·225	3·068 616	0·925	0·290 268	1·625	0·103 138
0·250	2·956 485	0·950	0·248 982	1·650	0·103 396
0·275	2·838 053	0·975	0·211 151	1·675	0·103 377
0·300	2·714 598	1·000	0·176 562	1·700	0·103 110
0·325	2·587 378	1·025	0·145 009	1·725	0·102 624
0·350	2·457 606	1·050	0·116 292	1·750	0·101 945
0·375	2·326 431	1·075	0·090 217	1·775	0·101 098
0·400	2·194 928	1·100	0·066 597	1·800	0·100 103
0·425	2·064 083	1·125	0·045 254	1·825	0·098 980
0·450	1·934 784	1·150	0·026 019	1·850	0·097 746
0·475	1·807 818	1·175	−0·008 731	1·875	0·096 418
0·500	1·683 870	1·200	+0·006 762	1·900	0·095 010
0·525	1·563 520	1·225	0·020 602	1·925	0·093 534
0·550	1·447 251	1·250	0·032 923	1·950	0·092 003
0·575	1·335 449	1·275	0·043 851	1·975	0·090 426
0·600	1·228 413	1·300	0·053 502	2·000	0·088 814
0·625	1·126 357	1·325	0·061 986	2·025	0·087 175
0·650	1·029 424	1·350	0·069 405	2·050	0·085 516
0·675	0·937 689	1·375	0·075 852	2·075	0·083 845
0·700	−0·851 167	1·400	+0·081 415	2·100	+0·082 166

TABLE 4

$P_0(\eta, \tau)$ *for Duplex Tunnels (Antisymmetrical)*

	η								
τ	0	0·05	0·10	0·15	0·20	0·25	0·30	0·35	0·40
0	0	0	0	0	0	0	0	0	0
0·05	0	0·009047	0·016566	0·021602	0·024035	0·024438	0·023746	0·022939	0·022875
0·10	0	0·016566	0·030650	0·040601	0·046041	0·047781	0·047377	0·046622	0·047223
0·15	0	0·021602	0·040601	0·055088	0·064347	0·068980	0·070656	0·071661	0·074491
0·20	0	0·024035	0·046041	0·064347	0·078027	0·087222	0·093264	0·098525	0·106169
0·25	0	0·024438	0·047781	0·068980	0·087222	0·102311	0·115091	0·127771	0·144140
0·30	0	0·023746	0·047377	0·070656	0·093264	0·115091	0·136818	0·160706	0·191733
0·35	0	0·022939	0·046622	0·071661	0·098525	0·127771	0·160706	0·200781	0·256546
0·40	0	0·022875	0·047223	0·074491	0·106169	0·144140	0·191733	0·256546	0·358616

TABLE 5

$P_1(\eta, \tau)$ for Duplex Tunnels (Antisymmetrical)

τ	η = 0	0·05	0·10	0·15	0·20	0·25	0·30	0·35	0·40
0	0	0	0	0	0	0	0	0	0
0·05	0	0·017921	0·032391	0·041355	0·044711	0·043895	0·041019	0·038147	0·037006
0·10	0	0·032391	0·059276	0·077102	0·085251	0·085730	0·082042	0·078025	0·077226
0·15	0	0·041355	0·077102	0·103172	0·118121	0·123398	0·122736	0·121122	0·124019
0·20	0	0·044711	0·085251	0·118121	0·141319	0·155127	0·162477	0·168730	0·181362
0·25	0	0·043895	0·085730	0·123398	0·155127	0·180398	0·201121	0·222717	0·255375
0·30	0	0·041019	0·082042	0·122736	0·162477	0·201121	0·240638	0·287766	0·358833
0·35	0	0·038147	0·078025	0·121122	0·168730	0·222717	0·287766	0·376754	0·524771
0·40	0	0·037006	0·077226	0·124019	0·181362	0·255375	0·358833	0·524771	0·853355

TABLE 6

$Q_0(\eta, \tau)$ for Duplex Tunnels (Symmetrical)

τ	η = 0	0·05	0·10	0·15	0·20	0·25	0·30	0·35	0·40
0	0·136778	0·132625$_5$	0·121077	0·104520	0·086030	0·068555	0·054415$_5$	0·045210	0·042008
0·05	0·132625$_5$	0·128927	0·118573	0·103554	0·086537	0·070223	0·056882$_5$	0·048212	0·045439
0·10	0·121077	0·118573	0·111404	0·100590	0·087746	0·074865	0·064019	0·057111$_5$	0·055808
0·15	0·104520	0·103554	0·100590	0·095597	0·088918	0·081542$_5$	0·075094	0·071615	0·073350
0·20	0·086030	0·086537	0·087746	0·088918	0·089393	0·089147	0·089138$_5$	0·091332$_5$	0·098558
0·25	0·068555	0·070223	0·074865	0·081542$_5$	0·089147	0·096989	0·105385	0·116081	0·132523
0·30	0·054415$_5$	0·056882$_5$	0·064019	0·075094	0·089138$_5$	0·105385	0·123932	0·146576	0·177970
0·35	0·045210	0·048212	0·057111$_5$	0·071615	0·091332$_5$	0·116081	0·146576	0·185820$_5$	0·242061
0·40	0·042008	0·045439	0·055808	0·073350	0·098558	0·132523	0·177970	0·242061	0·344541

TABLE 7

$Q_1(\eta, \tau)$ for Duplex Tunnels (Symmetrical)

τ	η = 0	0·05	0·10	0·15	0·20	0·25	0·30	0·35	0·40
0	0·292737	0·283965	0·259668	0·225073	0·186698	0·150467	0·120689	0·100012	0·090005
0·05	0·283965	0·276203	0·254519	0·223183	0·187770	0·153694	0·125240	0·105347	0·095996
0·10	0·259668	0·254519	0·239718	0·217216	0·190178	0·162543	0·138352	0·121223	0·114286
0·15	0·225073	0·223183	0·217216	0·206713	0·191989	0·174837	0·158526	0·147291	0·145909
0·20	0·186698	0·187770	0·190178	0·191989	0·191371	0·187972	0·183776	0·183212	0·193038
0·25	0·150467	0·153694	0·162543	0·174837	0·187972	0·200310	0·212658	0·229523	0·260434
0·30	0·120689	0·125240	0·138352	0·158526	0·183776	0·212658	0·246057	0·289880	0·359885
0·35	0·100012	0·105347	0·121223	0·147291	0·183212	0·229523	0·289880	0·376420	0·523737
0·40	0·090005	0·095996	0·114286	0·145909	0·193038	0·260434	0·359885	0·523737	0·851703

TABLE 8a

Calculated Interference for the Arrowhead Wing in N.P.L. Duplex Wind Tunnel. Lift, Rolling Moment and Pitching Moment

$$-\frac{(\Delta C_l)}{C_l'} \quad \text{for antisymmetrical loading (Appendix II, Table A 8)}$$

$$\left.\begin{aligned} &\frac{(\Delta\alpha)}{C_L'},\ \frac{(\Delta C_m)}{C_L'},\ -\frac{(\Delta C_l)}{C_L'} \ \text{[equations (7.5) and (7.6)]}\\ &\frac{(\delta C_L)}{C_L'} = \frac{\partial C_L}{\partial\alpha}\frac{(\Delta\alpha)}{C_L'} = 2\cdot732\,\frac{(\Delta\alpha)}{C_L'}\\ &\frac{(\delta C_l)}{C_l'} = \frac{C_L}{C_l}\left\{\frac{\partial C_l}{\partial\alpha}\cdot\frac{(\Delta\alpha)}{C_L'} - \frac{(\Delta C_l')}{C_L'}\right\}\\ &\qquad = \frac{2s}{\bar{y}'}\left\{0\cdot596\,\frac{(\Delta\alpha)}{C_L'} - \frac{(\Delta C_l')}{C_L'}\right\} \end{aligned}\right\}\ \text{for symmetrical loading}$$

Control span	$0\cdot\dot{3}\dot{6}s < y < s$		$0\cdot\dot{5}\dot{4}s < y < s$		$0\cdot\dot{7}\dot{2}s < y < s$		
Chord ratio	$E = 0\cdot2$	$E = 0\cdot4$	$E = 0\cdot2$	$E = 0\cdot4$	$E = 0\cdot2$	$E = 0\cdot4$	Uniform incidence
$-(\Delta C_l)/C_l'$	0·0230	0·0246	0·0202	0·0217	0·0188	0·0201	
$(\Delta\alpha)/C_L'$	0·0272	0·0296	0·0229	0·0252	0·0205	0·0227	0·0397
$(\Delta C_m)/C_L'$	0·0098	0·0096	0·0095	0·0094	0·0093	0·0093	0·0083
$-(\Delta C_l)/C_L'$	0·00065	0·00060	0·00085	0·00080	0·00095	0·00090	0·00010
$(\delta C_L)/C_L'$	0·0742	0·0809	0·0625	0·0688	0·0560	0·0621	0·1085
$\bar{y}'/s$	0·570	0·559	0·647	0·633	0·724	0·707	0·436
$(\delta C_l)/C_l'$	0·0591	0·0653	0·0448	0·0500	0·0364	0·0409	0·1090

TABLE 8b

Calculated Interference for the Arrowhead Wing in N.P.L. Duplex Wind Tunnel. Drag and Yawing Moment

$$(\delta C_D) = (\delta C_D)_a + (\delta C_D)_s \ \text{[equation (8.6)]}$$
$$(\Delta C_D) = -(\delta C_D) + 2\{\Delta C_l/C_l'\}(C_D')_a \ \text{[equation (8.9)]}$$
$$(\Delta C_n) = -(\delta C_n)_1 - (\delta C_n)_2 + 2\{\Delta C_l/C_l'\}C_n' \ \text{[equation (8.13)]}$$

For $(\delta C_n)_1$, γ_s corresponds to uniform incidence and γ_a to antisymmetrically deflected ailerons :
For $(\delta C_n)_2$, γ_s and γ_a correspond to symmetrically and antisymmetrically deflected ailerons respectively.

Control span	$0\cdot\dot{3}\dot{6}s < y < s$		$0\cdot\dot{5}\dot{4}s < y < s$		$0\cdot\dot{7}\dot{2}s < y < s$		
Chord ratio	$E = 0\cdot2$	$E = 0\cdot4$	$E = 0\cdot2$	$E = 0\cdot4$	$E = 0\cdot2$	$E = 0\cdot4$	Uniform incidence
$-(\delta C_D)_a/(C_l')^2$	0·179	0·180	0·159	0·161	0·150	0·151	
$-(\delta C_D)_s/(C_L')_2$	0·0248	0·0248	0·0221	0·0223	0·0220	0·0221	0·0255
$(\delta C_n)_1/(C_L')_1 C_l'$	0·0449	0·0437	0·0437	0·0426	0·0427	0·0418	
$(\delta C_n)_2/(C_L')_2 C_l'$	0·0435	0·0433	0·0437	0·0433	0·0456	0·0450	

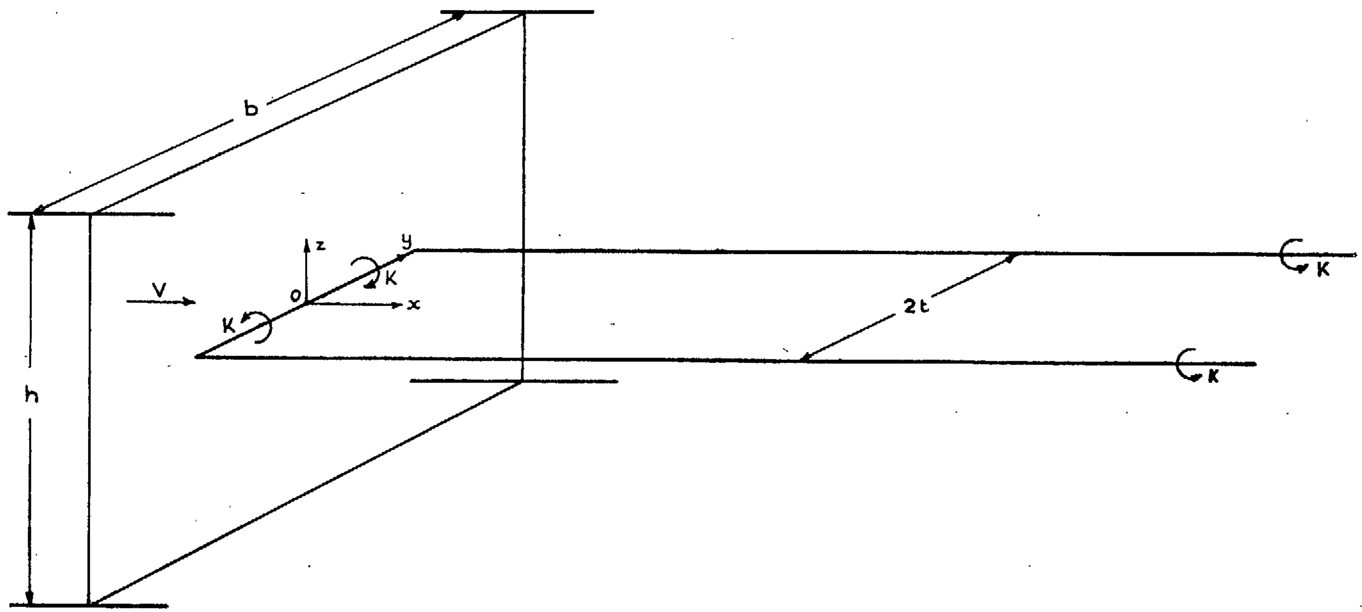

FIG. 1. Elementary vortex for antisymmetrical loading in a rectangular tunnel.

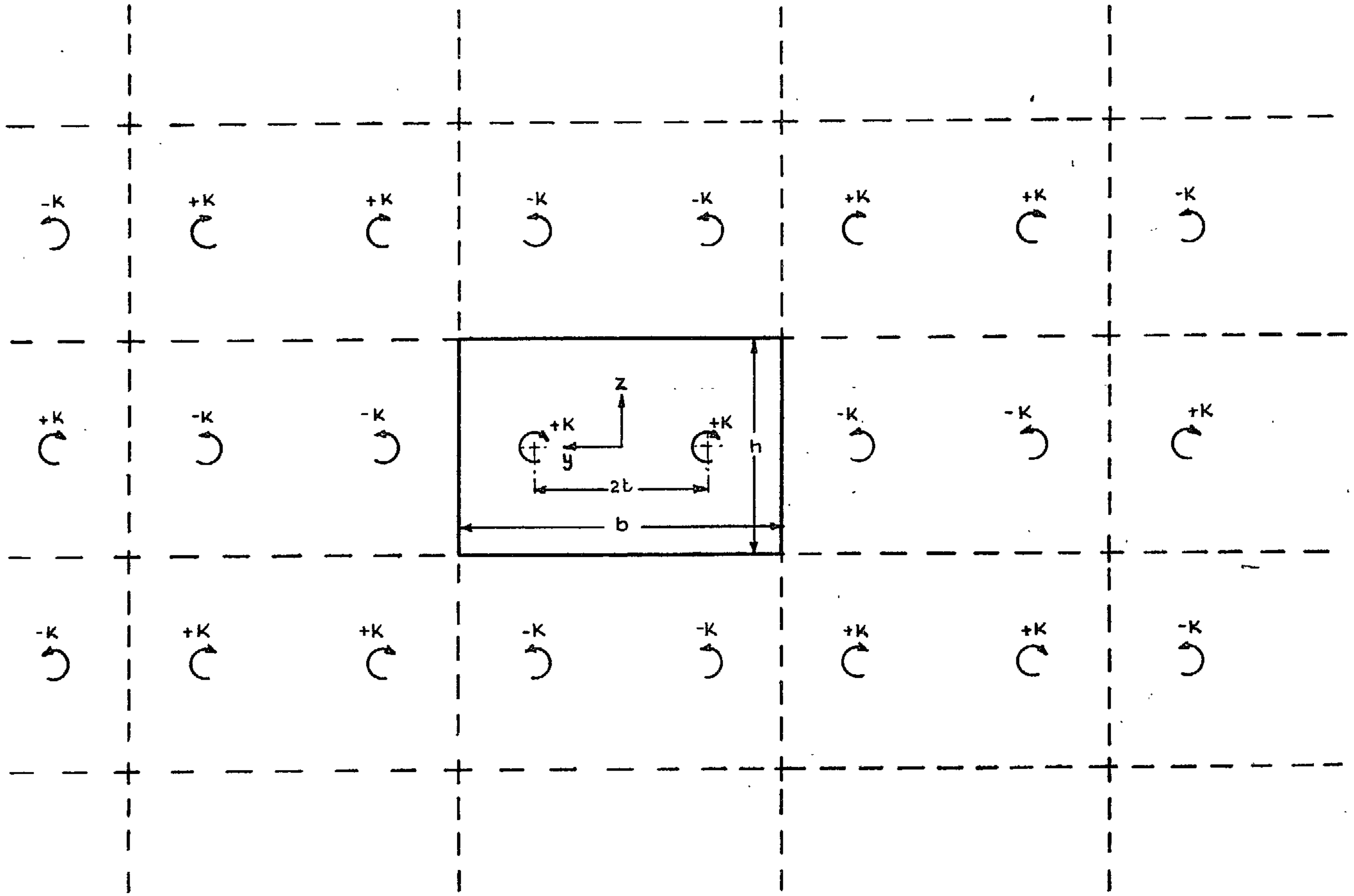

FIG. 2. Image system of antisymmetrical trailing vorticity.

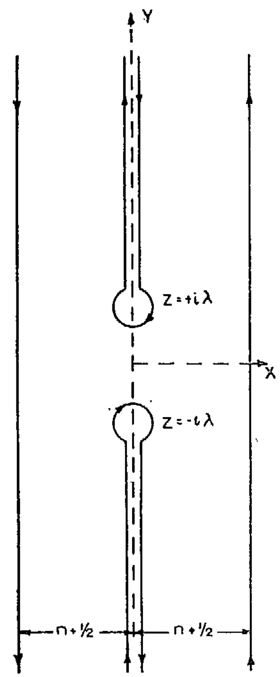

FIG. 3. Contour used for integration in Appendix I.

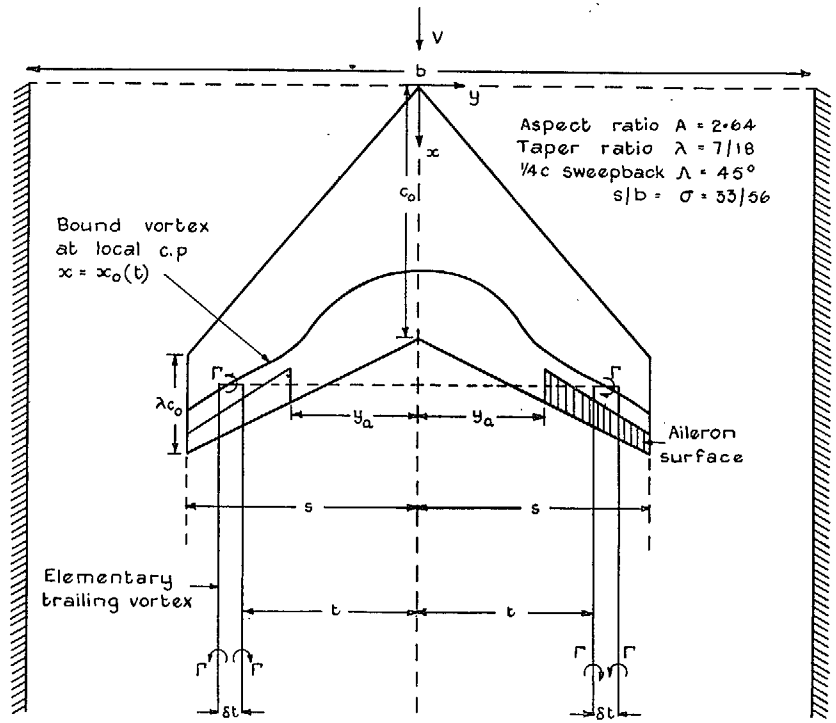

FIG. 4. Plan of the arrowhead wing with vorticity due to deflected ailerons.

I4359 Wt.19/8411 K7 12/55 D&Co. 34/263

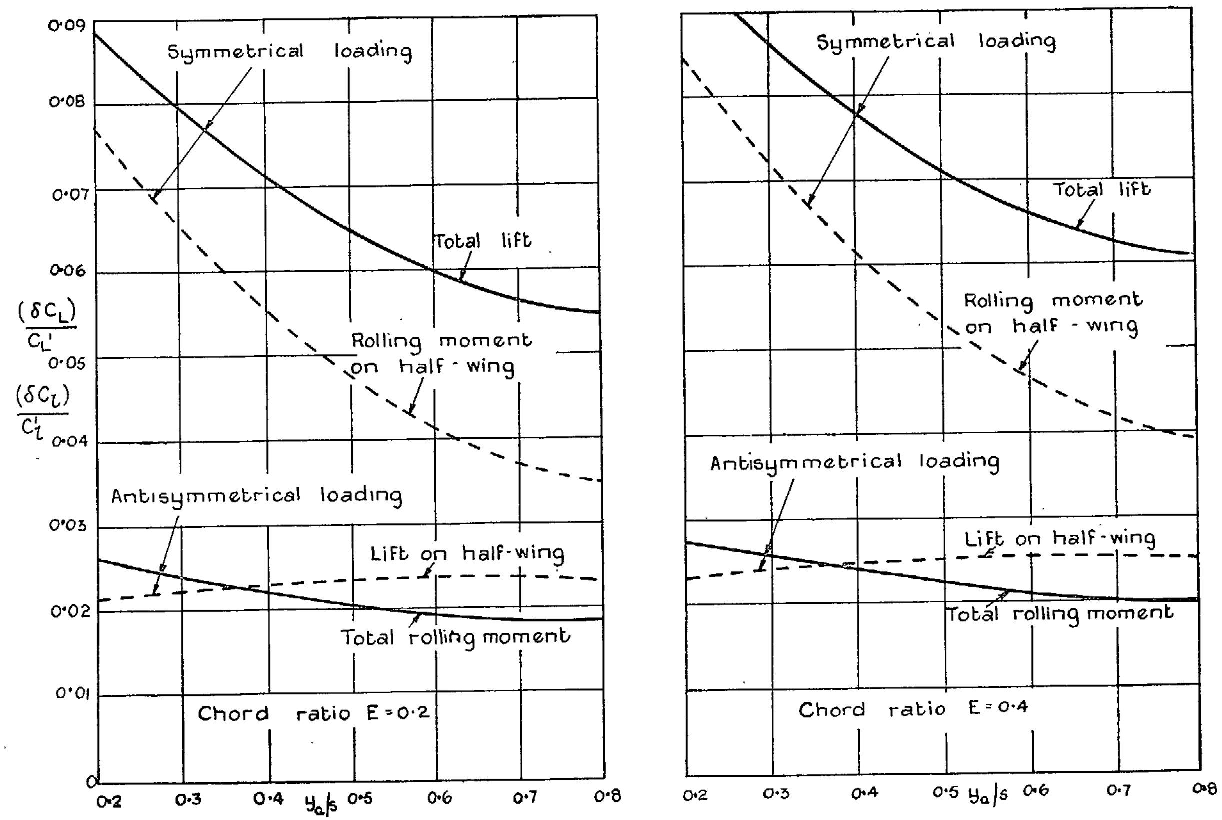

FIG. 5. Proportional interference corrections for the arrowhead wing with deflected ailerons in N.P.L. Duplex Wind Tunnel.

PRINTED IN GREAT BRITAIN

Publications of the Aeronautical Research Council

ANNUAL TECHNICAL REPORTS OF THE AERONAUTICAL RESEARCH COUNCIL (BOUND VOLUMES)

1939 Vol. I. Aerodynamics General, Performance, Airscrews, Engines. 50s. (51s. 9d.)
Vol. II. Stability and Control, Flutter and Vibration, Instruments, Structures, Seaplanes, etc. 63s. (64s. 9d.)

1940 Aero and Hydrodynamics, Aerofoils, Airscrews, Engines, Flutter, Icing, Stability and Control, Structures, and a miscellaneous section. 50s. (51s. 9d.)

1941 Aero and Hydrodynamics, Aerofoils, Airscrews, Engines, Flutter, Stability and Control, Structures. 63s. (64s. 9d.)

1942 Vol. I. Aero and Hydrodynamics, Aerofoils, Airscrews, Engines. 75s. (76s. 9d.)
Vol. II. Noise, Parachutes, Stability and Control, Structures, Vibration, Wind Tunnels. 47s. 6d. (49s. 3d.)

1943 Vol. I. Aerodynamics, Aerofoils, Airscrews. 80s. (81s. 9d.)
Vol. II. Engines, Flutter, Materials, Parachutes, Performance, Stability and Control, Structures. 90s. (92s. 6d.)

1944 Vol. I. Aero and Hydrodynamics, Aerofoils, Aircraft, Airscrews, Controls. 84s. (86s. 3d.)
Vol. II. Flutter and Vibration, Materials, Miscellaneous, Navigation, Parachutes, Performance, Plates and Panels, Stability, Structures, Test Equipment, Wind Tunnels. 84s. (86s. 3d.)

1945 Vol. I. Aero and Hydrodynamics, Aerofoils. 130s. (132s. 6d.)
Vol. II. Aircraft, Airscrews, Controls. 130s. (132s. 6d.)
Vol. III. Flutter and Vibration, Instruments, Miscellaneous, Parachutes, Plates and Panels, Propulsion. 130s (132s. 3d.)
Vol. IV. Stability, Structures, Wind tunnels, Wind Tunnel Technique. 130s. (132s. 3d.)

ANNUAL REPORTS OF THE AERONAUTICAL RESEARCH COUNCIL—

1937 2s. (2s. 2d.) 1938 1s. 6d. (1s. 8d.) 1939–48 3s. (3s. 3d.)

INDEX TO ALL REPORTS AND MEMORANDA PUBLISHED IN THE ANNUAL TECHNICAL REPORTS, AND SEPARATELY—

April, 1950 - - - - - - R. & M. No. 2600. 2s. 6d. (2s. 8d.)

AUTHOR INDEX TO ALL REPORTS AND MEMORANDA OF THE AERONAUTICAL RESEARCH COUNCIL—

1909–January, 1954 - - - - R. & M. No. 2570. 15s. (15s. 6d.)

INDEXES TO THE TECHNICAL REPORTS OF THE AERONAUTICAL RESEARCH COUNCIL—

December 1, 1936 — June 30, 1939.	R. & M. No. 1850.	1s. 3d. (1s. 5d.)
July 1, 1939 — June 30, 1945. -	R. & M. No. 1950.	1s. (1s. 2d.)
July 1, 1945 — June 30, 1946. -	R. & M. No. 2050.	1s. (1s. 2d.)
July 1, 1946 — December 31, 1946.	R. & M. No. 2150.	1s. 3d. (1s. 5d.)
January 1, 1947 — June 30, 1947. -	R. & M. No. 2250.	1s. 3d. (1s. 5d.)

PUBLISHED REPORTS AND MEMORANDA OF THE AERONAUTICAL RESEARCH COUNCIL—

Between Nos. 2251–2349. - -	R. & M. No. 2350.	1s. 9d. (1s. 11d.)
Between Nos. 2351–2449. - -	R. & M. No. 2450.	2s. (2s. 2d.)
Between Nos. 2451–2549. - -	R. & M. No. 2550.	2s. 6d. (2s. 8d.)
Between Nos. 2551–2649. - -	R. & M. No. 2650.	2s. 6d. (2s. 8d.)

Prices in brackets include postage

HER MAJESTY'S STATIONERY OFFICE

York House, Kingsway, London W.C.2; 423 Oxford Street, London W.1; 13a Castle Street, Edinburgh 2; 39 King Street, Manchester 2; 2 Edmund Street, Birmingham 3; 109 St. Mary Street, Cardiff; Tower Lane, Bristol 1; 80 Chichester Street, Belfast, *or through any bookseller*

S.O. Code No. 23-2948

R. & M. No. 2948